



D. De Lange

August, 2019

**Technology assessment and usability
study of a steerable needle prototype
as a tool in assisting percutaneous**

Technology assessment and usability study of a steerable needle prototype as a tool in assisting percutaneous liver interventions

by

D. de Lange

to obtain the degree of

Master of Science

In Biomedical Engineering

at the University of Technology in Delft,
to be defended publicly on Friday August 30, 2019 at 01:00 PM.



Thesis committee:

Dr. J.J. van den Dobbelsteen

TU Delft, chair, supervisor

Dr. Ir. N.J.P. van de Berg

TU Delft, supervisor

This thesis is confidential and cannot be published until August 1, 2021.

For an electronic version of this thesis visit <http://repository.tudelft.nl/>.

Preface

*There are no secrets to success.
It is the result of preparation, hard work,
and learning from failure.*

Colin Powell

During the writing of this thesis it is becoming more and more clear that this is the final step in completing the master Biomedical Engineering and obtaining the degree of “*Master of Science*”. Looking back at the past seven years of studying, for my master as well as for my bachelor, I’ve gained a lot of knowledge and experience. The human body was, besides technology, always of great interest for me and during the bachelor of Mechanical Engineering that I did, I noticed that I wanted to combine both fields of interest. The master Biomedical Engineering and the track Medical Instruments and Medical Safety (MIMS) connected well to my interests. I noticed that during the master courses I preferred projects with the goal of designing and/or testing of medical instruments.

In one of these courses, *Applied Experimental Methods*, I met my supervisor John van den Dobbelsteen and my daily supervisor Nick van de Berg. My internship, literature review and thesis project were all performed with their guidance and feedback, for which I want to express my gratitude. Nick in particular, while he gave me advice and helped me to tackle problems weekly during my internship, literature review and thesis project. Also, I would like to show my gratitude to interventional radiologist Adriaan Moelker from the Erasmus Medical Centre who helped me with obtaining subjects (also interventional radiologists) for one of the studies I performed, and gave feedback on my literature review with a medical point of view.

Furthermore I would like to thank my parents for helping me on a mental level and supporting me wherever they could throughout my bachelor and master studies.

*D. de Lange
Papendrecht, August 2019*

Inhoud

ABSTRACT.....	7
1. INTRODUCTION.....	7
2. USER STUDY AND EXPERIMENTAL TESTING OF THE INSTRUMENT CHANGE BETWEEN A STEERABLE AND RFA NEEDLE IN A PVA LIVER PHANTOM.....	10
2.1 INTRODUCTION.....	10
2.2 MATERIALS AND METHODS.....	10
2.2.1 MATERIALS.....	10
2.2.1.1 <i>Specimens</i>	10
2.2.1.2 <i>Targets</i>	11
2.2.1.3 <i>Instruments</i>	11
2.2.1.4 <i>Equipment</i>	11
2.2.2 METHODS.....	11
2.2.2.1 <i>Variables and constants</i>	11
2.2.2.2 <i>Experimental design</i>	11
2.2.2.3 <i>Experimental protocol</i>	13
2.2.2.4 <i>Subjects</i>	14
2.2.2.5 <i>Data processing</i>	14
2.3 RESULTS.....	14
2.3.1 TIME.....	14
2.3.2 SUCCESS RATE.....	15
2.3.3 QUESTIONNAIRE.....	16
2.4 DISCUSSION.....	17
3. DISPLACEMENT OF THE CANNULA TIP DUE TO INSTRUMENT CHANGE WITH A BIOPSY NEEDLE FOR A STRAIGHT AND CURVED TRAJECTORY.....	19
3.1 INTRODUCTION.....	19
3.2 MATERIALS AND METHODS.....	19
3.2.1 MATERIALS.....	19
3.2.1.1 <i>Specimens</i>	19
3.2.1.2 <i>Instruments</i>	19
3.2.1.3 <i>Equipment</i>	20
3.2.2 METHODS.....	20
3.2.2.1 <i>Variables and constants</i>	20
3.2.2.2 <i>Experimental design</i>	20
3.2.2.3 <i>Experimental protocol</i>	21

3.2.2.4 Data processing.....	22
3.3 RESULTS.....	22
3.3.1 RESULTS DEFLECTION.....	23
3.3.2 RESULTS DISPLACEMENT.....	23
3.4 DISCUSSION.....	23
4. DISCUSSION.....	25
5. ABBREVIATIONS.....	27
6. REFERENCES.....	28

APPENDICES

I: LITERATURE REVIEW.....	30
II: TUMOR DEVELOPMENT STUDY.....	49
III: MANUAL USER STUDY.....	59
IV: INFORMED CONSENT (DUTCH).....	61
V: QUESTIONNAIRE (DUTCH).....	62
VI: RAW DATA USER STUDY.....	64
VII: RAW DATA OF CANNULA DISPLACEMENT STUDY.....	69

Abstract

PURPOSE. The purpose of this thesis is to investigate the possibility of implementing a prototype of a steerable needle in a medical procedure. Therefore the two main research questions are: “Can the intended user perform a steering motion with the steerable needle and reach the target area following a straight and curved trajectory?” and “Does the tip of the cannula maintain its position after the instrument change with a biopsy needle for a straight and curved trajectory?”.

METHODS. Two studies were conducted to answer these research questions. A user study was designed and performed to test the steering properties of the steerable needle for a straight and curved trajectory. A second controlled study with automated insertions was designed and performed to investigate the cannula tip displacement after the instrument change.

RESULTS. The results of both studies show that steering towards a specific target is highly achievable with the steerable needle for insertions with a straight and curved trajectory. Results also show a high success-rate, a low time consumption for the instrument change, and a high satisfactory level on the manual handling of the steerable needle by the interventional radiologists. The results of the second study show that the cannula tip maintains its position after the instrument change for a straight trajectory, and the cannula tip only displaces 1.4 mm back over a deflection of ± 25 mm after the instrument change for a curved trajectory.

CONCLUSION. Reaching the target with a steering motion is achievable with the steerable needle and only a small displacement of the cannula tip is seen after the instrument change for a maximum imposed curved trajectory. These results answer the main questions concerning the effectivity of the steerable needle and are promising for future implementation of this prototype in a real medical procedure, containing real patients, and real liver tissue.

KEY WORDS. liver disease – liver biopsy – radiofrequency ablation – steerable needle – polyvinyl alcohol

1. Introduction

The liver is one of the largest organs in the human body. It plays a central role in all the metabolic processes that occur inside the body, filters the blood, stores nutrients, produces bile, supports the blood in the production of clotting factors, and is vital for many more life functions [1-4]. Hepatic diseases can be dangerous or even fatal for the patient, while it affects the efficiency of the liver and thereby the vital functions. There are many diseases that can affect the liver such as hepatitis, fatty liver disease, cirrhosis, liver cancer, etc [1, 5]. Diagnosis and treatment of hepatic diseases is necessary to maintain and restore the vital functions of the liver.

Liver biopsy is required to make a diagnosis, determine the prognosis, and make

decisions concerning a treatment plan for these hepatic diseases [6,7]. It is one of the many diagnostic tools, but is seen as the golden standard and has been a cornerstone in evaluating and managing patients with hepatic diseases [6, 8-12]. Hepatitis B [11], hepatitis C [13], hepatocellular carcinoma (HCC) [14], and nonalcoholic fatty liver disease/nonalcoholic steatohepatitis (NAFLD/NASH) [12, 15] are examples of hepatic diseases that depend on liver biopsy for optimal disease treatment and management. Hepatic tissue can be obtained with different liver biopsy methods. The percutaneous method is the most widely used method [9]. It introduces a long needle through the skin, subcutaneous tissues, intercostal muscles between the ribs, and peritoneum into the liver and removes a small piece of liver

tissue [16]. Local anesthesia is used and tissue diagnosis of hepatic diseases is achieved without subjecting the patient to the greater risk of general anesthesia and laparotomy used in open surgery [17].

Treatment of hepatic diseases can be achieved in several ways and depends on the diagnosis that is made. These treatments can vary from modifying the lifestyle of the patient to performing a liver transplant [1, 2, 18]. Percutaneous Radiofrequency ablation (RFA) is one of the treatment procedures that is used to control liver cancer by destructing cancerous cells. This minimally invasive technique is used as an alternative therapy for HCC and liver metastases if surgical resection or a transplant cannot be performed. It introduces a needle percutaneously to the tumor (target tissue) and destroys the tumor without harming the surrounding liver tissue [19, 20]. Radiofrequency energy flows through the electrodes in the tip of the RFA needle and creates ionic agitation. This ionic agitation results in heat which causes destruction of the cancerous cells [21-23].

To accurately diagnose and effectively treat hepatic diseases it is necessary to place the needle tip of both biopsy and RFA needle at the desired target tissue in order to obtain a biopsy or destruct tissue cells. The needle needs to be retracted and inserted again if the needle tip is not placed accurately at the lesion or target tissue. Insertion of the needle to the target liver tissue is called a 'pass'. Studies have shown that the complication rate increases when the number of passes increases for percutaneous liver biopsies, which is not desirable [24, 25]. A similar outcome is expected for increasing the number of passes for RFA needles. Therefore it is highly recommended to reduce the number of passes for both biopsy and RFA needle in order to make proper diagnosis and effectively treat hepatic diseases, without further harming the patient.

A needle with a steerable tip could reduce the number of passes of both needles, while one can actively steer towards the tumor or target liver tissue using ultrasound imaging technique. However, no commercially available steerable needle is yet present. A prototype of a steerable needle has been

developed at the Technical University of Delft by Nick van de Berg. The tip of this steerable needle is able to achieve a steering motion by actively varying the tip angle. The tip angle can be changed manually between 0° and 11° by means of a lever. A cannula surrounds the shaft of the steerable needle, that maintains its position after the steerable needle is retracted when the target area is reached. This cannula creates a free path to the target area for a straight stiff needle that fulfills a different function which is not achievable by the steerable needle itself, such as ablation or taking a biopsy.

The purpose of this thesis is to investigate the possibility of implementing the prototype of a steerable needle in a medical procedure. Therefore it is necessary to thoroughly test the needle in artificial liver tissue, made with Polyvinyl alcohol (PVA), that mimics real liver tissue [26]. In order to perform ablation to or take a biopsy from the target tissue it is of great importance that the steerable needle reaches the target tissue accurately, and the straight stiff needle is positioned at the target tissue after the instrument change. Therefore the two main research questions are: "Can the intended user perform a steering motion with the steerable needle and reach the target area following a straight and curved trajectory?" and "Does the tip of the cannula maintain its position after the instrument change with a straight stiff biopsy needle for a straight and curved trajectory?". A user study was designed involving interventional radiologists from the Erasmus Medical Centre in order to answer the first main research question. An ethics commission gave permission to conduct this study. Three secondary objectives that were investigated in this study were: the execution time of the entire instrument change, the success-rate of hitting the target after the instrument change, and the satisfactory level on the manual handling of the steerable needle by the interventional radiologists. A second study was designed in a controlled environment with automated insertions in order to answer the second research question concerning the displacement of the cannula tip after the instrument change. Furthermore, a literature review was

Chapter 1

conducted, concerning liver biopsy adequacy in relation to needle gauge and needle tip type, in order to investigate the definition of liver biopsy adequacy, give an overview of the different needles that are used to obtain liver biopsies, and to determine which biopsy needle achieves the most adequate biopsy specimens. This literature review is presented in Appendix I. At last, an additional study was performed concerning the development of PVA tumor targets in PVA liver phantoms which is presented in Appendix II.

2. User study and experimental testing of the instrument change between a steerable and RFA needle in a PVA liver phantom

2.1 Introduction

A user study was designed to investigate if it is possible to perform a steering motion with the steerable needle and reach the target area following a straight and curved trajectory in order to create a free path for a straight stiff RFA needle. This was the primary objective of this study. The RFA needle does not contain steering properties and fulfils a function to the target tissue that is not achievable by the steerable needle. It is also necessary to gain insight in the execution time of the entire instrument change, the success-rate of hitting the desired target tissue with the RFA needle after the instrument change, and the manual handling of the steerable needle by clinicians. Therefore three secondary objectives were investigated with this user study:

- The time it took to reach the desired target with a RFA needle after creating a free trajectory with the steerable needle.
- The success-rate of reaching the target with the RFA needle.
- The satisfactory level of the interventional radiologists on the working principle of the steerable needle, the manageability of the steerable needle, and the duration of the entire task.

2.2 Materials and methods

In the following section a detailed description will be given concerning the materials that were used for the experiment, the experimental set-up and the method that was used in conducting the experiment.

2.2.1 Materials

2.2.1.1 Specimens

It is important to use a specimen which resembles the properties of real cirrhotic liver tissue. Polyvinyl Alcohol (PVA), is a synthetic polymer that is soluble in water. The liver phantom gets a heterogeneous structure, comparable with a real liver, when it is made with PVA. The liver phantom that was used for this experiment was made with PVA (SELVOL™, Sekisui Specialty Chemicals America, Dallas, Texas) and coolant (CAREX, Burg Group B.V., Heerhugowaard, Netherlands) containing a mass fraction of 5% PVA and three freeze-thaw cycles. The values for the mass fraction and the number of freeze-thaw cycles were chosen after a few trials and interventional radiologist Adriaan Moelker from the Erasmus Medical Centre confirmed that the density of the phantom resembled the density of the cirrhotic livers their dealing with in real-life RFA procedures. The mixture of the PVA was poured into a plastic case with dimensions 120 mm x 110 mm x 200 mm. In order to make a PVA liver phantom you need to follow a particular recipe that is stated below.

1. Take the PVA particles that account for 5% of the mass and a liquid containing 60% water and 40% coolant which accounts for 95% of the mass and mix it together.
2. Pour this mixture of PVA, water and coolant in a beaker and stir (with help of a magnetic stirrer) while heating the mixture up to 95 °C. Keep stirring it for 10 minutes at 95 °C.
3. Pour the solution into the plastic case and keep it for a few hours at room temperature so that air bubbles leave the solution and the overall

- temperature of the mixture decreases to 50 °C.
4. Put the mold for 12-24 hours in the freezer at a temperature of -20 °C.
 5. Take the phantom out of the freezer and keep it at room temp for another 12-24 hours.

Points 3 till 5 account for one freeze-thaw cycle. Repeat until desired number is reached.

2.2.1.2 Targets

Targets were created inside the PVA phantom by placing three aluminum rods in longitudinal direction in the plastic case before the PVA mixture was poured in. These rods were removed after completing the freeze-thaw cycles, creating three longitudinal holes in the PVA phantom that were filled with water during the experiment. Water is clearly distinguishable from the PVA phantom with ultrasound imaging, which is of great importance for the subjects while image guidance is used to steer the steerable needle towards the targets. Figure 1 shows the placement of the rods in the case and shows the PVA phantom after removal of the rods.

2.2.1.3 Instruments

A current prototype of a steerable needle (figure 2) was used to perform the first part of the experiment where the steerable needle was inserted in the PVA phantom towards the target. The working principle of the steering mechanism of the steerable needle is shown in figure 3. The needle is surrounded by a removable cannula that maintains its position in the PVA phantom after the steerable needle is retracted, creating a free trajectory for the RFA needle. The cannula can be removed by twisting the Luer-lock as is shown in figure 4. A 17G 200 mm RFA probe (HS AMICA RFH 17200E 25V1, HS Hospital Services, Roma, Italy) with diamond tip was used to conduct the second part of the experiment, where the RFA needle is inserted through the cannula towards the target.

2.2.1.4 Equipment

A self-made aluminium frame with trocars was used to create a fixed position and insertion angle of 90° for the steerable and RFA

needle above the PVA phantom liver. Trocars are often used in medical procedures while it functions as a portal for the placement of other instruments. An Ultrasound system (iU22 xMatrix - DS, Phillips Healthcare, Eindhoven, Netherlands) was used to follow the trajectory and to detect the tip location of the needles. The MeVisLab 2.7.1 (VC12-64) application was used to capture the ultrasound images from the Phillips ultrasound machine. A stopwatch was used to time each part of the experiment. The experimental setup is shown in figure 5.

2.2.2 Methods

A carefully designed experiment was set up concerning the instrument change between a steerable needle and a RFA needle. A lot of factors were taken in consideration. A strict protocol was written and all the needed materials were investigated.

2.2.2.1 Variables and constants

The time to fulfill the experiment and the accuracy of reaching the target are the dependent variables. The independent variable is the subject performing the experiment. The only constants that remain are:

- | | |
|-----------------------|---|
| - Specimen: | PVA |
| - Needle type: | 18G steerable needle and 17G RFA needle |
| - Initial distance: | 0 mm |
| - Insertion depth: | ±100 mm |
| - Angle of insertion: | 90° |
| - Temperature: | 20 °C |
| - Pressure: | 760 mmHG |

2.2.2.2 Experimental design

Two experiments were performed by each of the six subjects. The first experiment contained six punctures with the steerable needle following a straight trajectory to the target and the second experiment contained six punctures with the steerable needle following a curved trajectory. A total of 72 insertions were performed by the six subjects combined.

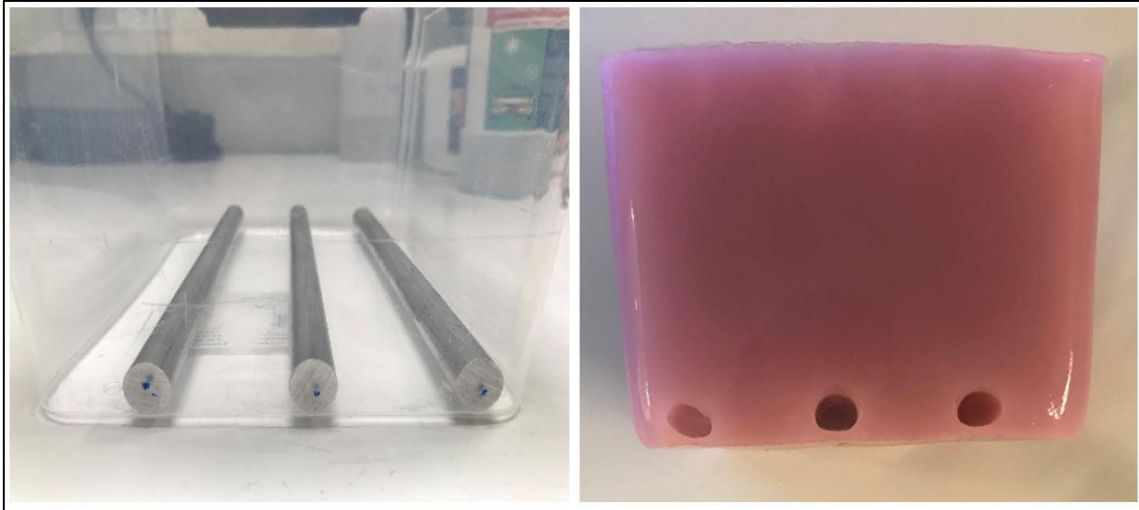


Figure 1: Aluminum rods placed in longitudinal direction in the plastic case before PVA mixture is poured in (left), aluminum rods removed after freeze-thaw cycles were completed, creating hollow targets in the PVA phantom that were filled with water during the experiment (right).

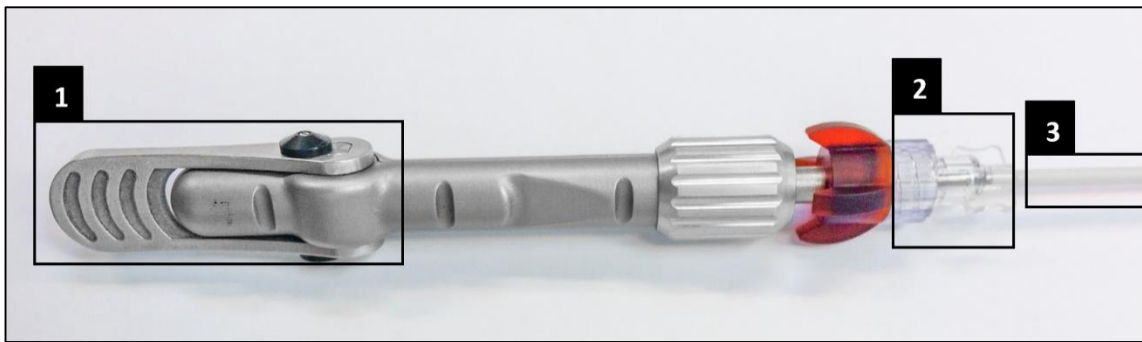


Figure 2: Prototype of a steerable needle with: 1; the steering mechanism using a lever, 2; attachment of the cannula to the steerable needle by means of a Luer-lock, 3; plastic cannula surrounding the shaft of the steerable needle.



Figure 3: Steering mechanism of the steerable needle. Turning the lever clockwise results in a clockwise rotation of the needle tip and vice versa for turning the lever counter clockwise.

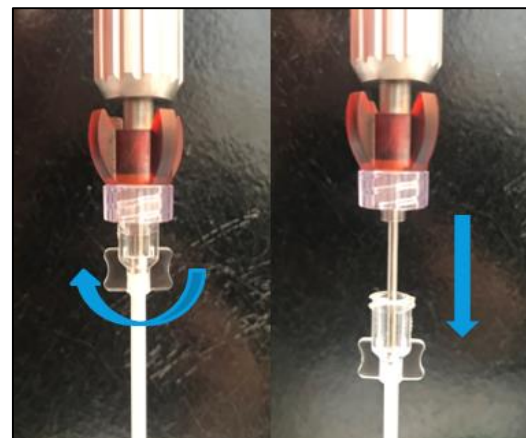


Figure 4: Detachment of the cannula from the steerable needle by twisting the Luer-lock in clockwise direction

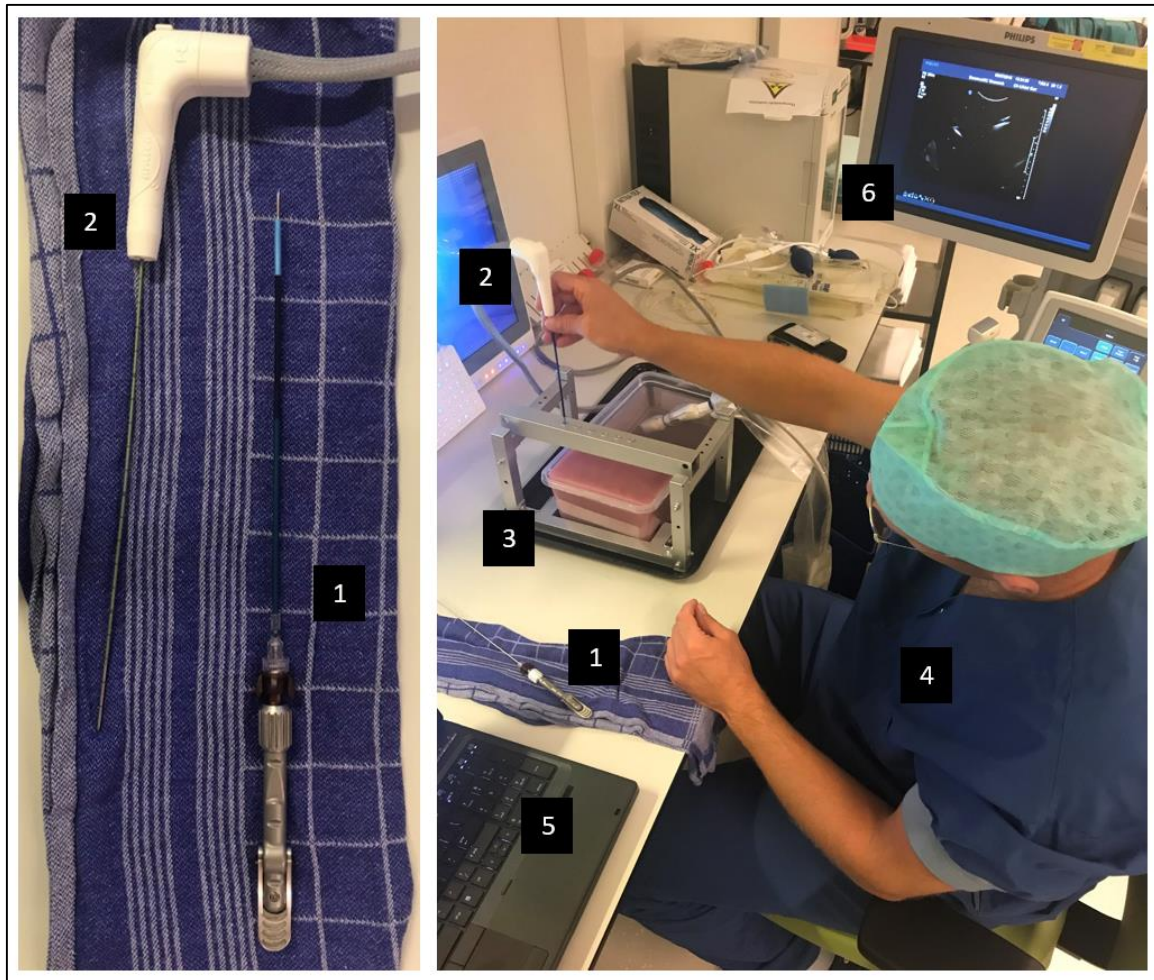


Figure 5: Experimental setup with: 1; Prototype of the steerable needle, 2; the RFA needle, 3; aluminum frame with the PVA phantom, 4; one of the subjects performing the experimental tasks, 5; Laptop to note the time and save the images from the ultrasound imaging device, 6; ultrasound imaging device.

2.2.2.3 Experimental protocol

A Dutch user manual, supported with images, was provided to the subjects before the experiment (Appendix III) as well as a Dutch informed consent form (Appendix IV). The working principle of the steerable needle and the experimental protocol were explained in the user manual and subjects were able to get acquainted with the device before the experiment started. To begin the experiment all the materials needed to be present and everything had to be calibrated and put in place.

The first step was for the subject to insert the steerable needle through the trocar into the PVA phantom to the desired location (target). The needle tip location was checked by means of ultrasound imaging technique and the

experimenter noted if the needle hit or missed the desired target. The time was also noted after

the steerable needle reached the target. Then the subject retracted the steerable needle, after unlocking the Luer lock of the steerable needle, leaving the cannula inside the PVA phantom. The RFA needle is then inserted through the cannula into the PVA phantom, following the trajectory that was made by the steerable needle, to the target. The needle tip location of the RFA needle was checked by means of ultrasound imaging technique and the experimenter noted again if it was a hit or a miss. The time between hitting the target with the steerable needle and hitting the target with the RFA needle was noted by the experimenter.

A questionnaire (Appendix V) was presented to the subjects at the end of the experiments.

2.2.2.4 Subjects

The subjects were interventional radiologists working at the Erasmus MC in Rotterdam. Each of the subjects worked with RFA needles or had experience with similar medical procedures. Six interventional radiologists performed the experiment and their age differed from 34 to 43 years. They all performed similar procedures before and years of experience differed from 3 to 9 years.

2.2.2.5 Data processing

In order to detect the needle hitting or missing the target it was necessary to estimate the location of the needle tip. In some cases, the needle or its reverberations (imaging artifacts) could obscure the targets, complicating a hit/miss estimate. Encircling the target with a line and drawing a line on the shaft of the needle on the ultrasound image can determine more clearly if it hits or misses the target.

2.3 Results

2.3.1 Time

For a full overview of the experimental results concerning the raw time measurements, see Appendix VI. The experiment was divided into two parts. The first part started with puncturing the PVA phantom and ended when the steerable needle reached the target. The second part started with retraction of the steerable needle from the PVA phantom and ended with reaching the target with the RFA needle. Table 1 indicates the time it took to fulfil the two separate tasks as well as the time it took to fulfil the entire experiment (two tasks combined) when following a straight trajectory to the target. Table 2 indicates the time it took to fulfil the two separate tasks as well as the time it took to fulfil the entire experiment when following a curved trajectory to the target.

Figure 6 shows the learning curves in terms of time required of the experiment with the straight and curved trajectory. The mean

Table 1: Mean \pm standard deviation of the time to complete the total task and two separate tasks per subject performing a straight trajectory.

Straight trajectory	Time to complete the first part (s)	Time to complete the second part (s)	Total time (s)
Subject 1	17.58 \pm 2.88	30.51 \pm 5.16	48.09 \pm 6.52
Subject 2	19.53 \pm 3.60	24.38 \pm 4.88	43.91 \pm 6.41
Subject 3	19.38 \pm 15.49	23.00 \pm 3.63	41.98 \pm 18.1
Subject 4	6.98 \pm 0.86	25.46 \pm 8.21	32.44 \pm 7.97
Subject 5	13.92 \pm 2.54	17.43 \pm 7.20	31.35 \pm 8.81
Subject 6	17.86 \pm 6.19	23.16 \pm 6.17	41.03 \pm 11.43
Average time of subjects	15.87 \pm 8.20	22.02 \pm 7.21	37.89 \pm 12.22

Table 2: Mean \pm standard deviation of the time to complete the total task and two separate tasks per subject performing a curved trajectory.

Curved trajectory	Time to complete the first part (s)	Time to complete the second part (s)	Total time (s)
Subject 1	11.48 \pm 25.69	32.02 \pm 5.86	68.22 \pm 30.26
Subject 2	26.55 \pm 11.30	27.54 \pm 7.39	54.10 \pm 13.49
Subject 3	13.13 \pm 3.39	14.59 \pm 1.90	27.73 \pm 3.85
Subject 4	17.70 \pm 15.54	28.27 \pm 7.20	45.98 \pm 18.9
Subject 5	9.73 \pm 2.26	12.67 \pm 2.55	22.37 \pm 3.91
Subject 6	27.61 \pm 16.32	16.57 \pm 2.21	44.10 \pm 16.10
Average time of subjects	21.82 \pm 17.38	21.94 \pm 9.11	43.75 \pm 22.98

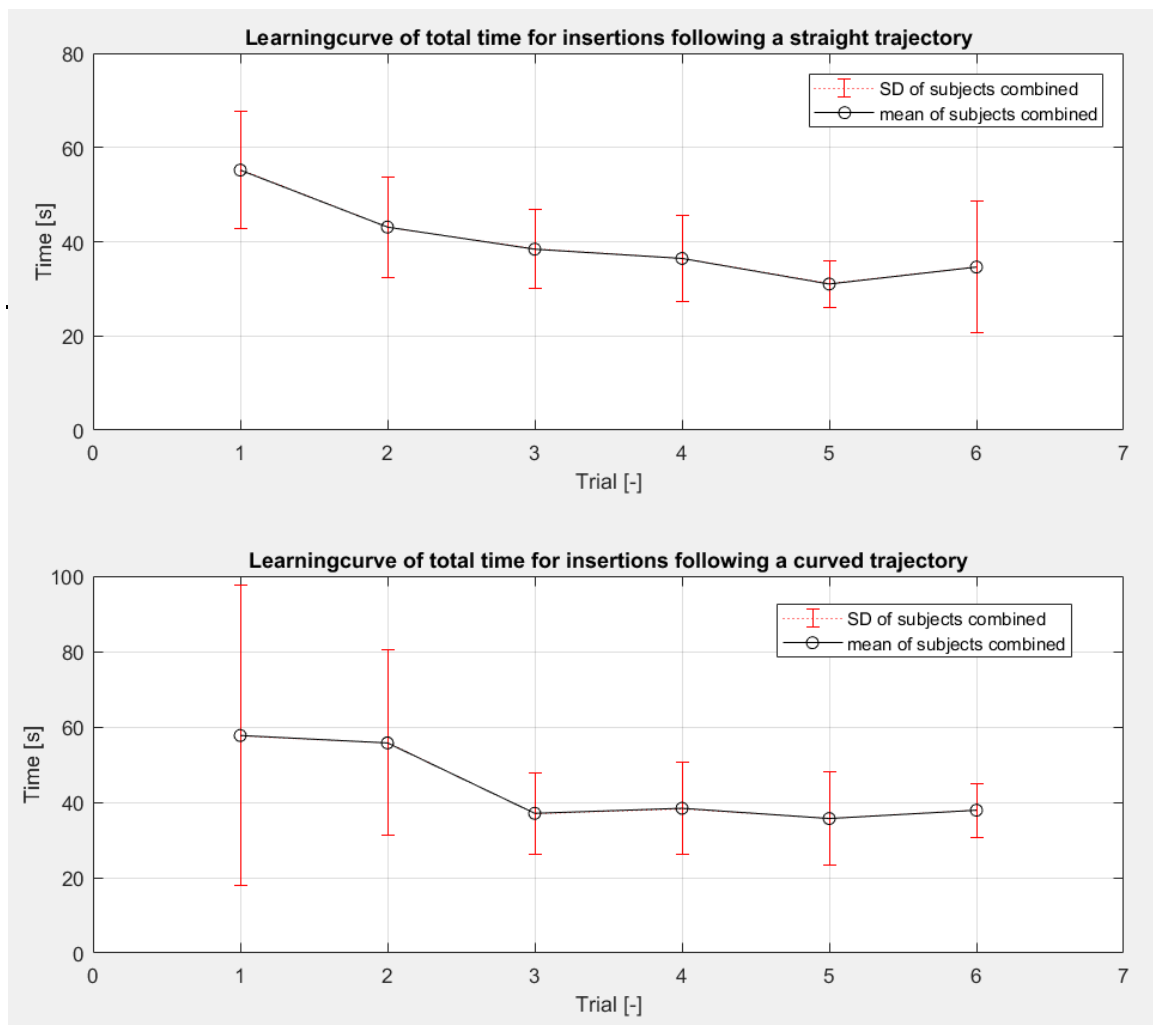


Figure 6: Learning curves for insertions with the straight trajectory (upper graph) and curved trajectory (lower graph). The black circles represent the mean total time of the six subjects combined for each trial. The red bars show the standard deviations of the six subjects combined for each trial.

(black circles) and standard deviation (red bars) of the total time of the six subjects combined is plotted against the number of trials. The total time decreases when the number of performances increases until a certain point where stability is reached. This indicates the presence of a learning effect. The total time seems to get stable after the 1st performance for the straight trajectory and after the 2nd performance for the curved trajectory.

2.3.2 Success rate

The hit-miss ratio was estimated using a binary numeral system with two numbers: 1 and 0. Number 1 indicates a hit which means that the needle is located inside the target. The edge of the target is also considered a hit.

Number 0 indicates a miss, which means that the needle is located outside the target. A total of 72 insertions were performed by the subjects. Six insertions, three with a straight trajectory and three with a curved trajectory, were excluded from quantitative analyses, due to occurrence of measurements errors or inaccessible data. The success-rate per needle for each trajectory is shown in table 3. For a full overview of the experimental results concerning the hits and misses of each needle, see Appendix VI.

The targets were reached in the first attempt, without retracting and replacing the needle, in 59 out of the 66 measurements that were used for quantitative analyses. The other

Table 3: Hit-miss ratio of the steerable needle and the RFA needle with a straight and curved trajectory.

	Hit (1)	Miss(0)	Success-rate(%)
Straight trajectory (33)			
Steerable needle	33	0	100%
RFA needle	33	0	100%
Curved trajectory (33)			
Steerable needle	33	0	100%
RFA needle	30	3	90.9%

seven measurements did not reach the target in the first attempt and used two (3x), three (3x) or four (1x) attempts to reach the target. These multiple attempts only occurred in the experiment with the needle following a curved trajectory.

2.3.3 Questionnaire

The questionnaire that was given at the end of the experiment can be found in Appendix V. The questionnaire consists of seven statements and one open-ended question. The statements had to be answered with a score ranging from one to five, one being bad and five being excellent. The open-ended question had to be answered freely without giving a score. The following seven statements and one open-ended question were presented:

- I. The weight of the steerable needle is easy to handle during the experiment
 - II. The steering mechanism (lever) and the disconnection of the Luer lock are quickly mastered
 - III. Steerability of the needle in the PVA phantom liver.
 - IV. Course of the instrument change during the experiment.
 - V. Time needed to go through the different steps of the task (Long = 1, short = 5).
 - VI. Integration possibility of the steerable needle in a real medical procedure.
 - VII. Overall experience with the experiment.
- Open What should the steerable needle cost in your opinion?

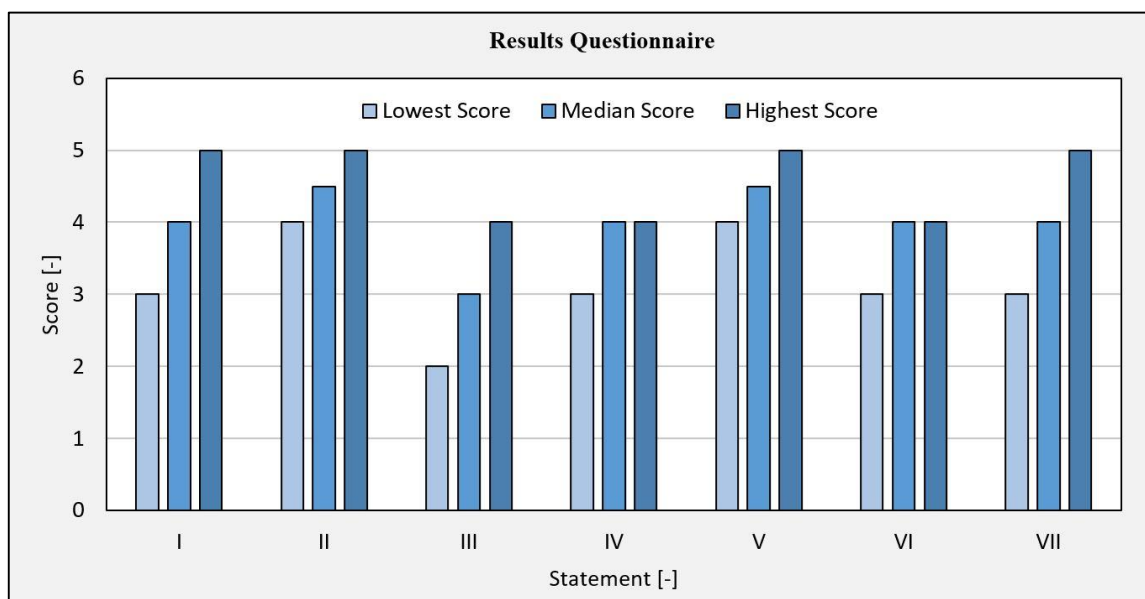


Figure 7: Histogram that shows the lowest, median, and highest score given by the six subjects for each of the seven statements of the questionnaire.

The scores of the seven statements are represented in the histogram presented in figure 7.

The answers of the subjects to the open-ended question of the questionnaire differed between €50,- and €200,- for a disposable steerable needle and between €1500,- and €2000,- for a sterilisable steerable needle. Two subjects did not have an opinion about the price in this stadium.

2.4 Discussion

The primary objective of this study was to investigate if it is possible to steer towards a target with a steerable needle in order to create a free trajectory for a straight stiff needle. There were three secondary objectives in this user study that were also investigated: the time it took to perform the entire task of switching between instruments and reaching the target with the RFA needle; the success-rate of reaching the target with the RFA needle after the instrument change; and the satisfactory level of the subjects (interventional radiologists) on the working principle of the steerable needle, the manageability of the steerable needle and the duration of the entire task.

The results on the time to complete the entire task show that the mean total time of the subjects combined was 39.8 seconds for the straight trajectory and 43.8 seconds for the curved trajectory. So the mean total time to insert the steerable needle to the target, perform the instrument change, and insert the RFA needle through the cannula to the target was performed in less than a minute for both trajectories. The total time per performance decreased when the number of performances increased until a certain stability was reached which indicates that a learning effect is present. The high standard deviation of the mean total time can be explained by the differences between the subjects in years of experience, age and working approach. Some subjects tend to take their time to reach the target with both needles while others subjects execute the tasks in a fast manner. This can cause a larger spread in the time data.

The results on the success-rate of both needles hitting the target show a success-rate of 100% for both the steerable needle and the RFA needle for a straight trajectory. The success-rate for the curved trajectory was 100% and 90.9% for the steerable and RFA needle respectively. This indicates a perfect success-rate for the straight trajectory and a very high success-rate for the curved trajectory. The lower success-rate of the RFA needle for a curved trajectory can be explained by straightening of the cannula due to the stiffness of the RFA needle. This can result in missing the target if the target is not hit in the centre with the steerable needle but at the edge of the target. Some subjects did not reach the target within the first attempt for a curved trajectory and retracted the steerable needle in order to steer earlier to the target. This can be explained by the fact that the subjects needed to get acquainted in the first performances with the steering technique of the needle. This also explains the multiple attempts that occurred for insertions following a curved trajectory.

The results of the questionnaire show a high satisfactory level on the working principle and the manageability of the steerable needle as well as the duration of the entire task. The opinions of the subjects on the steerability in the PVA phantom scored lower. This can be explained by the soft structure of the PVA phantom which caused the steerable needle to be pushed straight down for a few insertions instead of steering with a curved trajectory to the target. The PVA phantom was out of the fridge during the entire experiment, while no fridge was directly available at the location of the experiment, causing it to get softer due to the room temperature after the first two subjects performed the experiments.

The targets in this study were cavities which were filled with water during the experiment, these targets are not comparable to real tumors. These cavities were in some cases compressed when inserting the needle through the PVA phantom. Forces on the needle were probably different while water provides different friction to the needle tip and shaft compared to the PVA tissue. An additional study concerning the development of PVA

tumor targets in a PVA liver phantom was performed and is presented in Appendix II.

In conclusion, steering towards a specific target is highly achievable with the steerable needle as we can see from the success-rate. The success-rate of hitting the target is 100% for the steerable needle when performing a straight and curved trajectory. The success-rate of the RFA needle hitting the target after the instrument change was 100% and 90.9% for the straight and curved trajectory respectively. The entire task of steering with the steerable needle to the target, switching between instruments and placing the RFA needle through the cannula to the desired target can be achieved in less than a minute causing a low time consumption. The satisfactory level of the interventional radiologists on the working principle and the manageability of the steerable needle as well as the duration of the entire task was high. Together with the high success-rate and the low time consumption this will increase the possibility of integration of the steerable needle in real medical procedures.

3. Displacement of the cannula tip due to instrument change with a biopsy needle for a straight and curved trajectory

3.1 Introduction

Steering to a desired target area is clearly achievable with the steerable needle for a straight and a curved trajectory as is seen from the results of chapter 2. However reaching the target area is only the first part of the procedure. A displacement of the cannula tip after the instrument change was seen from the results of chapter 2. It is of great importance that the tip of the straight stiff needle, fulfilling a different function than the steerable needle is able to achieve, is positioned at the target after the instrument change. Therefore, a second study is designed to investigate the relevance of this effect. The aim of this study is to answer the question: “Does the tip of the cannula maintain its position after the instrument change with a straight stiff needle for a straight and curved trajectory?”. The results of chapter 2 on the success-rate of hitting the desired target showed a perfect success-rate (100%) of hitting the target after the instrument change for the straight trajectory and a high success-rate (90.9%) of hitting the target after the instrument change for a curved trajectory. This shows that the stiffness of a straight stiff needle probably effects the curvature of the cannula. Therefore the hypothesis is that the tip location of the cannula will not change for a straight trajectory and that it will change for a curved trajectory when inserting a straight stiff biopsy needle. A carefully designed experiment was set up to test this hypothesis and answer the main question by means of measuring the deflection of the cannula before the instrument change and the displacement of the cannula tip after the instrument change with a biopsy needle for a straight and curved trajectory.

3.2 Materials and Methods

In the following section a detailed description will be given concerning the materials that were used for the experiment, the experimental set-up and the method that was used in conducting the experiment.

3.2.1 Materials

Different specimens, instruments and equipment were needed for this experiment to succeed and to get results concerning cannula tip displacement during the instrument change.

3.2.1.1 Specimens

The liver phantom that was used for this experiment was made with Polyvinyl Alcohol (SELVOL™, Sekisui Specialty Chemicals America, Dallas, Texas) and coolant (CAREX, Burg Group B.V., Heerhugowaard, Netherlands) containing a mass fraction of 4% PVA and two freeze-thaw cycles. This particular mass fraction was used while insertions into PVA phantoms with a mass fraction of 4% and two freeze-thaw cycles are comparable to a healthy human liver in terms of estimated friction along the needle shaft and the number of peak forces [26]. This mixture was poured into an acryl case with dimensions 130 mm x 130 mm x 220 mm. In order to make a PVA phantom you need to follow the same recipe as is stated in section 2.2.1.1 using a mass fraction of 4% PVA instead of 5% PVA and using two instead of three freeze-thaw cycles.

3.2.1.2 Instruments

The steerable needle has an adjustable tip angle which can vary between 0° and 11° . Needles with fixed angles were used instead of the steerable needle to minimize the effect of deviation in the angle of the steerable tip during the experiment. The needles that were used in this experiment were a straight 1.04 mm (19G) nitinol stylet with a 0° angle and diamond tip, a 1.04 mm (19G) nitinol stylet with a fixed 11° angle and diamond tip, and a 20 mm 18G biopsy needle (HS NOTA18200, HS Hospital Services, Roma, Italy) with a bevel tip and rapid firing mechanism. A nitinol cannula was placed over the stylets, that maintained its position in the PVA phantom after retraction of the stylet, to create a free trajectory for the biopsy needle. Figure 8 shows an overview of the needles and the cannula used in this experiment.

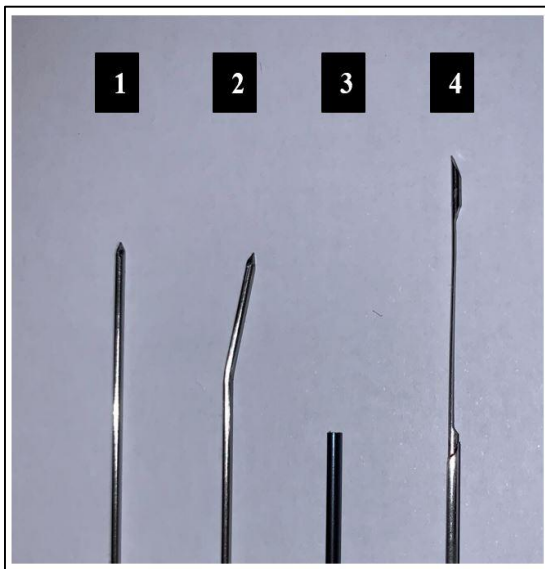


Figure 8: 1; 19G nitinol stylet with 0° diamond tip, 2; 19G nitinol stylet with 11° diamond tip, 3; nitinol cannula, 4; 18G biopsy needle with bevel tip and rapid firing mechanism.

3.2.1.3 Equipment

A linear stage (EGSL-BS-55-250-12.7P, Festo, Esslingen am Neckar, Germany) was used to clamp the nitinol stylets with cannula and insert them horizontally into the PVA phantom with a constant speed and insertion depth. An acryl case with same dimensions as the acryl case mentioned in

section 3.2.1.1 was designed with Solidworks and cut-out with a laser cutter. It contained 50 puncture holes on the insertion-side of the case and an open structure with rulers, in order to read the coordinates of the tip of the cannula, on the other side where the stylet exits the PVA phantom. Lab-Jack (Cenco-Lerner, Breda, Netherlands) was used to translate the acryl case with PVA phantom in horizontal and vertical direction. A camera (Iphone XR, California, USA) with a resolution of 12.0 megapixels was used to capture the tip location of the cannula, when exiting the PVA phantom, in order to determine the displacement of the cannula. The experimental set-up is shown in figure 9.

3.2.2 Methods

To test the hypothesis a carefully designed experiment was set up concerning the displacement of the cannula tip. A lot of factors are taken in consideration. A strict protocol was written and all the needed materials were investigated.

3.2.2.1 Variables and constants

For the research question it is necessary to measure the displacement of the tip of the cannula between insertion with the stylet and insertion with the biopsy needle. The displacement is the dependent variable. For the independent variable the tip angle is taken, which differs between 0° and 11° . The only constants that remain are:

- Velocity	= 20 mm/s
- Specimen	= PVA
- Needle type	= 19G stylet and 18G biopsy needle
- Initial distance	= 0 mm
- Insertion depth PVA	= 130 mm
- Angle of insertion	= 90°
- Temperature	= 20°C
- Pressure	= 760 mmHG

3.2.2.2 Experimental design

For the experiment two different needle angles for the stylet were used, which resulted in two different experimental

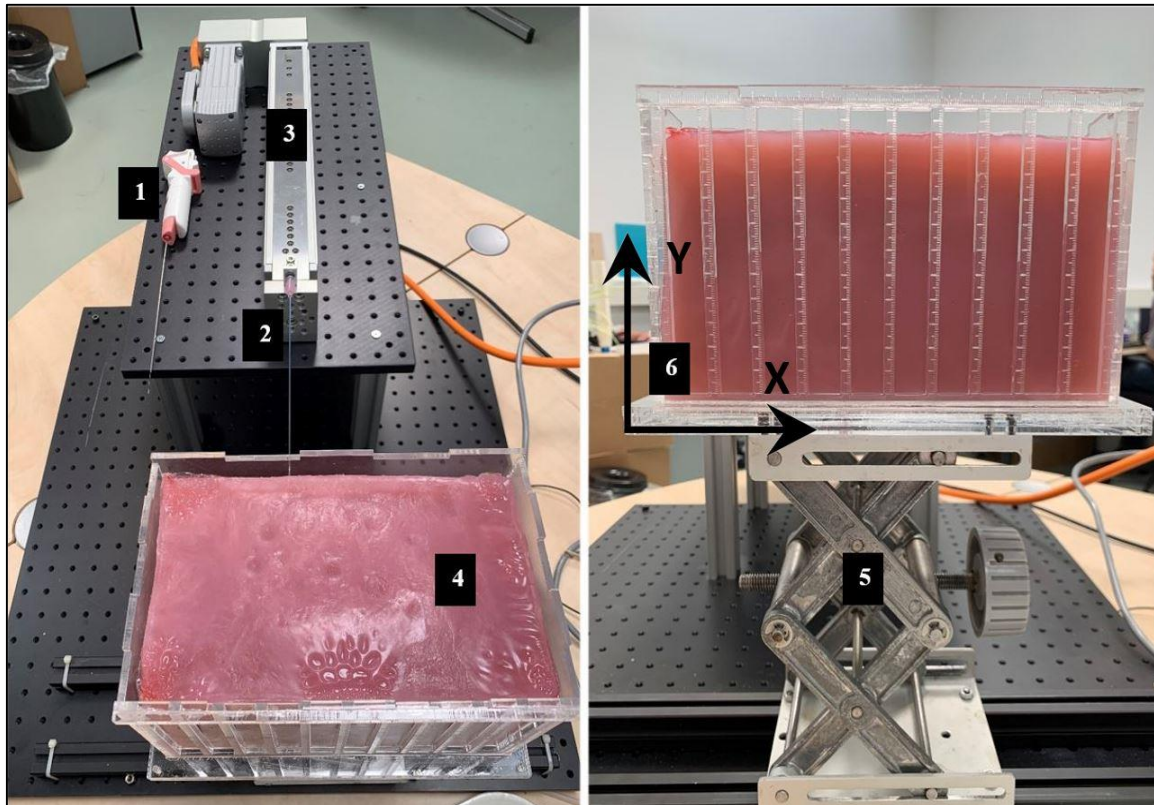


Figure 1: Experimental set-up with 1; 18G biopsy needle, 2; nitinol stylet with nitinol cannula clamped on the linear stage, 3; linear stage, 4; PVA liver phantom, 5; Lab-Jack which can move the PVA phantom vertically and horizontally, 6; acryl case which contains 50 puncture holes on the insertion-side and an open structure with rulers on the other side where the stylet exits the PVA phantom.

conditions. Each experimental condition was tested for 50 repetitions. This makes a total of 100 repetitions for the two stylets combined. The acryl case that holds the PVA phantom in place during the experiment, contains 50 puncture holes, therefore two PVA phantoms were needed to fulfill the 100 repetitions. Both PVA phantoms were punctured for 25 repetitions with the 0° stylet and 25 repetitions with the 11° stylet.

3.2.2.3 Experimental protocol

To begin the experiment all the materials needed to be present and everything had to be calibrated and put in place. First of all the begin position, velocity and insertion depth of the needle were implemented in the computer that controls the linear stage. The stylet with cannula had to be aligned with one of the puncture holes of the acryl case. The

stylet with the 11° angle was placed with the curvature facing upwards (positive y-direction). This is done by translating the acryl case in both the horizontal and vertical direction with the Lab-Jack. A test run without PVA phantom was done before each puncture to see if the stylet followed a straight path through the case. The stylet with cannula was then positioned in the insertion hole of the acryl case by means of the jog motion of the linear stage. The stylet with cannula was inserted by the linear stage until the implemented insertion depth was reached. The stylet tip and tip of the cannula penetrated the PVA phantom and were clearly visible on the other side of the acryl case. Coordinates of the tip of the cannula were noted and a picture was taken. The stylet was then retracted by the linear stage while the cannula stayed in place. After that, the biopsy needle was manually inserted through the cannula until the tip reached the end location.

Coordinates of the tip of the cannula were noted again and a picture was taken. The displacement and deflection of the cannula was then determined based on the x- and y-coordinates of the tip location of the cannula and its location of entrance of the PVA phantom.

3.2.2.4 Data processing

Displacement of the cannula due to instrument change was determined by the difference in x- and y-coordinates between the tip location of the cannula after insertion with the stylet and the tip location of the cannula after inserting the biopsy needle through the cannula.

$$d_x = x_{can_biopsy} - x_{can_stylet} \quad (1)$$

$$d_y = y_{can_biopsy} - y_{can_stylet} \quad (2)$$

Where d_x and d_y are the displacement in mm of the cannula in x- and y-direction respectively. Furthermore x_{can_biopsy} and y_{can_biopsy} are the x- and y-coordinates of the tip location of the cannula after inserting the biopsy needle through the cannula and x_{can_stylet} and y_{can_stylet} are the x- and y-coordinates of the tip of the cannula after insertion of the stylet with cannula.

The deflection of the cannula was determined by the difference in x- and y-coordinates between the location of entrance of the cannula in the PVA phantom and the tip location of the cannula after insertion with the stylet.

$$D_x = x_{can_stylet} - x_{can_entrance} \quad (3)$$

$$D_y = y_{can_stylet} - y_{can_entrance} \quad (4)$$

Where D_x and D_y are the deflection in mm of the cannula in x- and y-direction respectively. Furthermore $x_{can_entrance}$ and $y_{can_entrance}$ are the x- and y-coordinates of the location where the cannula enters the PVA phantom.

3.3 Results

For a full overview of the raw experimental results concerning the deflection and the displacement in x- and y-direction for each insertion see Appendix VII. The deflection and the displacement are plotted in both x- and y-direction of each insertion with the 0° and the 11° stylet in figure 10.

The data in figure 10 shows the different relationships between the deflection and displacement of the cannula obtained from the experiment but does not give an insight in the spread of the data. Therefore boxplots of the displacement and deflection of the cannula in

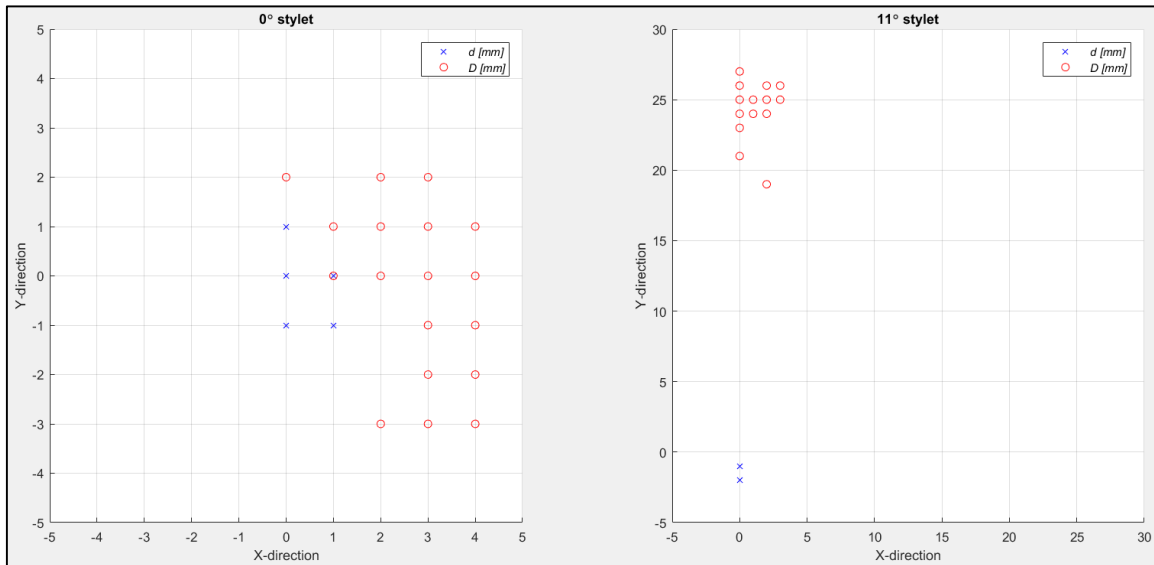


Figure 10: Deflection (D) and displacement (d) of the nitinol cannula in both x- and y-direction for each insertion with the 0° stylet (l) and the 11° stylet (r). Both needle plots contain 50 data points for the displacement and 50 data points for the deflection. Some points overlap.

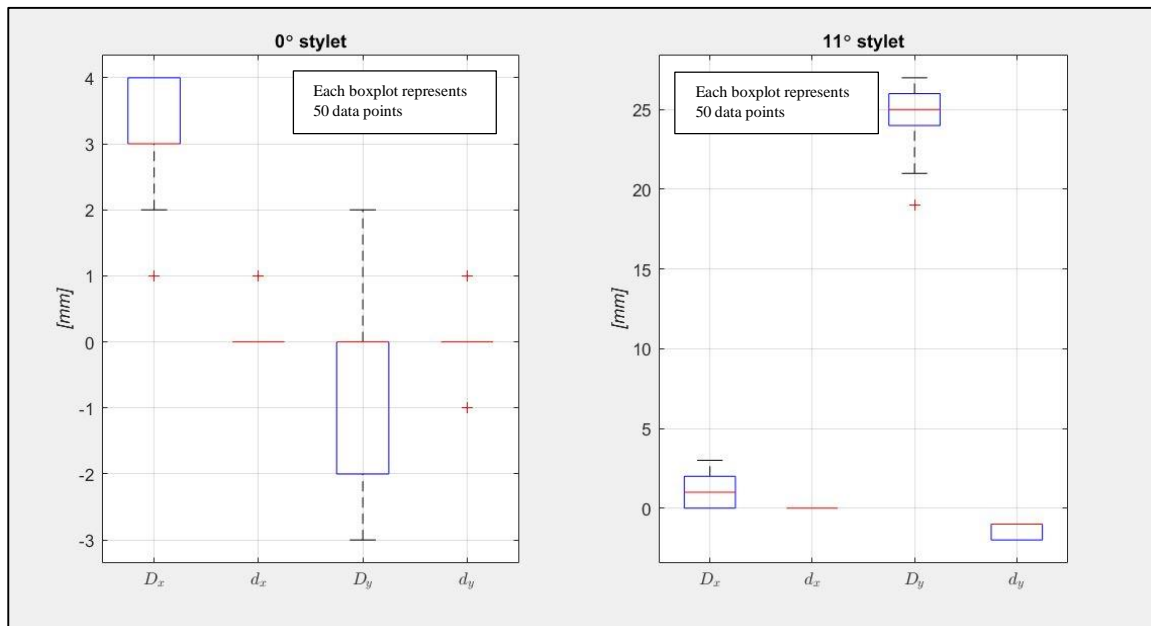


Figure 2: Boxplots of the deflection (D) and the displacement (d) in the x- and y- direction for the 0° stylet (l) and the 11° stylet (r). Each boxplot represents 50 data points.

the x- and y- direction for both stylets are plotted in figure 11.

3.3.1 Results Deflection

Most of the insertions with the 0° stylet ($\pm 75\%$) had a deflection between 3 and 4 mm in the x-direction while $\pm 50\%$ had a deflection in the y-direction between 0 and -2 mm for an insertion depth of 130 mm. The median and mean deflection in the x-direction were 3 and 3.16 mm respectively, while it was 0 and -0.46 mm in the y-direction.

Most of the insertions with the 11° stylet ($\pm 75\%$) had a deflection between 0 and 2 mm in the x-direction while $\pm 50\%$ of the insertions had a deflection in the y-direction between 24 mm and 26 mm for an insertion depth of 130 mm. The median and mean deflection in the x-direction were 1 and 1.12 mm respectively, while it was 25 and 24.76 mm in the y-direction.

3.3.2 Results displacement

Almost all of the insertions with the 0° stylet had a displacement of the cannula tip of 0 mm in the x- and y-direction. The median and mean displacement in the x-direction were 0 and 0.04 mm respectively, while they were both 0 mm in the y-direction.

All the insertions with the 11° stylet had a displacement of the cannula tip of 0 mm in the x-direction and between -1 and -2 mm in the y-direction. The median and mean displacement in the x-direction were both 0 mm, while it was -1 and -1.4 mm in the y-direction. In this case, the negative sign means that the cannula is less deflected after insertion with the biopsy needle compared to the deflection of the cannula after insertion with the stylet.

3.4 Discussion

The aim of this experiment was to test the hypothesis by investigating the displacement of the tip of the cannula during instrument change with a straight stiff biopsy needle. This was done for a nitinol cannula following a straight trajectory using a stylet with a 0° angle and for a curved trajectory using a stylet with a fixed 11° angle.

The results for the insertions following a straight trajectory with the 0° stylet showed an overall mean displacement of the tip of the cannula of 0.04 mm in the x-direction and 0 mm in the y-direction for a mean deflection of 3.16 mm and -0.46 mm in the x- and y-direction, respectively. Meaning that the cannula tip does not displace from its original

location during the instrument change for an insertion with a straight trajectory.

The results for the insertions following a curved trajectory with the 11° stylet showed an overall mean displacement of the tip of the cannula of 0 mm in the x-direction and -1.4 mm in the y-direction for a mean deflection of 1.12 mm and 24.76 mm in the x- and y-direction, respectively. Meaning that the cannula tip only shifts back in the y-direction, compared to its original location, during the instrument change for an insertion with a curved trajectory.

The deflections that occurred for the insertions with a straight trajectory could be explained by the fact that the cannula did not perfectly enclose the stylets. The cannula needed to fit around both the stylets and the biopsy needle, while the stylets were 19G and the biopsy needle was 18G. This results in more friction between the 0° stylet with enclosed cannula and the PVA phantom. This is less visible for the curved trajectory because the angle of the 11° stylet has a larger influence on the deflection. Another factor that can explain these deflections is the heterogeneous properties of the PVA phantom.

Future research is needed in order to see if a biopsy needle is able to obtain an adequate biopsy sample of the target tissue after the instrument change with the steerable needle. A literature review was conducted, concerning liver biopsy adequacy in relation to needle gauge and needle tip type. This review was conducted in order to investigate the definition of liver biopsy adequacy, give an overview of the different needles that are used to obtain liver biopsies, and to determine which biopsy needle achieves the most adequate biopsy specimens. This literature review is presented in Appendix I.

In conclusion, practically no displacement of the cannula tip occurs for a controlled straight insertion in both x- and y-direction, and no displacement occurs in the x-direction while only a very small displacement occurs in the y-direction for a controlled maximum steering motion during an insertion of 130 mm. This means that the hypothesis was true. So with large curvatures of the stylet, that are actually not aspired to achieve in real-life with the steerable needle, only a very small

displacement of the cannula tip occurs after instrument change with a straight stiff biopsy needle. Which means that the displacement of the cannula only tends to get closer to zero for tip angles smaller than 11° of the steerable needle. These are promising results, while such small displacements are manageable and can be taken into account during future medical procedures with the steerable needle.

4. Discussion

The goal of this thesis was to investigate the possibility of implementing the prototype of a steerable needle, designed by Nick van de Berg, in a medical procedure involving real liver tissue and real patients. Therefore the two main research questions were: “Is it possible to perform a steering motion with the steerable needle and reach the target area following a straight and curved trajectory?” and “Does the tip of the cannula maintain its position after the instrument change with a straight stiff needle for a straight and curved trajectory?”. Two studies were designed to answer these research questions. A user study was designed involving interventional radiologists from the Erasmus Medical Centre in order to answer the first research question. Three secondary objectives that were investigated in this study were: the execution time of the entire instrument change, the success-rate of hitting the target after the instrument change, and the satisfactory level on the manual handling of the steerable needle by the interventional radiologists. A different study was designed in a controlled environment in order to answer the second research question concerning the displacement of the cannula tip after the instrument change.

Results from the first study show that steering towards a specific target is highly achievable with the steerable needle when looking at the success-rate of hitting the targets. The success-rate of hitting the target is 100% for the steerable needle when performing a straight and curved trajectory. The success-rate of the straight stiff RFA needle hitting the target after the instrument change was 100% and 90.9% for the straight and curved trajectory respectively. The entire task of steering with the steerable needle to the target, switching between instruments and placing the straight stiff RFA needle through the cannula to the desired target can be achieved in less than a minute causing a low time consumption. The satisfactory level of the interventional radiologists on the working principle and the

manageability of the steerable needle as well as the duration of the entire task was high.

Results from the second study show practically no displacement of the cannula tip for a straight trajectory in both x-and y-direction, and no displacement occurs in the x-direction while only a very small displacement occurs in the y-direction for a curved trajectory. The average maximum deflection of the needle following a curved trajectory was 24.76 mm over a distance of 130 mm. The straight stiff biopsy needle straightened the cannula after the instrument change in such a way that the average deflection of the cannula was 1.4 mm less than before the instrument change. So with large curvatures of the stylet, that are actually not aspired to achieve in real-life with the steerable needle, only a very small displacement of the cannula tip occurs after instrument change with a straight stiff biopsy needle. Which means that the displacement of the cannula only tends to get closer to zero for tip angles smaller than 11° of the steerable needle. These are promising results, while such small displacements are manageable and can be taken into account during future medical procedures with the steerable needle.

Both studies used different straight stiff needles. The first study used a 17G RFA needle while the second study used a 18G biopsy needle. Both needles will have a different stiffness due to their difference in diameter and difference in material of the needle. Also, the cannula used in the first study is made of plastic while the cannula in the second study is made of nitinol. This can be explained by the fact that the steerable needle was in an earlier design stage during the design of the user study. The goal always was to use a nitinol cannula for the final product of the steerable needle, therefore a nitinol cannula was used in the second study. At last, the density of the PVA liver phantoms is different, while the first study concerned cirrhotic livers and the second study concerned healthy liver tissue. It is assumed that the results from both

studies are generalizable for both biopsy and RFA needles.

In conclusion, the results of both studies show that steering towards a specific target is highly achievable with the steerable needle for insertions with a straight and curved trajectory, the cannula tip maintains its position after the instrument change for a straight trajectory, and the cannula tip only displaces 1.4 mm back over a deflection of ± 25 mm after the instrument change for a curved trajectory. Together with the high success-rate, the time consumption of less than a minute for the instrument change, and the high satisfactory level on the manual handling of the steerable needle by the interventional radiologists, this will increase the possibility of integration of the steerable needle in real medical procedures. More research is still needed before this prototype of the steerable needle can actually be implemented. However these results are promising results that will aid in the implementation of this prototype of a steerable needle in a real medical procedure, containing real patients, and real liver tissue.

5. Abbreviations

G	gauge
HCC	hepatocellular carcinoma
NAFLD	nonalcoholic fatty liver disease
NASH	nonalcoholic steatohepatitis
PVA	polyvinyl alcohol
RFA	radiofrequency ablation

6. References

- Newman T. (2018, March 2). What does the liver do?. Retrieved from: <https://www.medicalnewstoday.com/articles/305075.php>
- Malignant Hepatic (liver) Lesions. (2018, June 13) Retrieved from: <https://my.clevelandclinic.org/health/diseases/14628-malignant-hepatic-liver-lesions>
- How does the liver work? (2016, August 22). Retrieved from: <https://www.ncbi.nlm.nih.gov/books/NBK279393/>
- Liver: Anatomy and Functions. (n.d.). Retrieved from: <https://www.hopkinsmedicine.org/health/conditions-and-diseases/liver-anatomy-and-functions>
- Raypole C. (2019, March 21). Liver diseases 101. Retrieved from: <https://www.healthline.com/health/liver-diseases>
- Rockey, D. C., Caldwell, S. H., Goodman, Z. D., Nelson, R. C., & Smith, A. D. (2009). Liver biopsy. *Hepatology*, 49(3), 1017-1044.
- Sherman, M., & Bruix, J. (2015). Biopsy for liver cancer: How to balance research needs with evidence-based clinical practice. *Hepatology*, 61(2), 433-436.
- Campbell, M. S., & R. Reddy, K. (2004). The evolving role of liver biopsy. *Alimentary pharmacology & therapeutics*, 20(3), 249-259.
- Pineda, J. J., Diehl, D. L., Miao, C. L., Johal, A. S., Khara, H. S., Bhanushali, A., & Chen, E. Z. (2016). EUS-guided liver biopsy provides diagnostic samples comparable with those via the percutaneous or transjugular route. *Gastrointestinal endoscopy*, 83(2), 360-365.
- Lefkowitz J.H. (2015). Scheuer's Liver Biopsy Interpretation E-Book: Elsevier Health Sciences.
- Mani, H., & Kleiner, D. E. (2009). Liver biopsy findings in chronic hepatitis B. *Hepatology*, 49(S5), S61-S71.
- Brunt, E. M. (2001). Nonalcoholic steatohepatitis: definition and pathology. In *Seminars in liver disease* (Vol. 21, No. 01, pp. 003-016). Copyright© 2001 by Thieme Medical Publishers, Inc., 333 Seventh Avenue, New York, NY 10001, USA. Tel.:+ 1 (212) 584-4662.
- Dienstag, J. L. (2002). The role of liver biopsy in chronic hepatitis C. *Hepatology*, 36(S1), S152-S160.
- Caturelli, E., Solmi, L., Anti, M., Fusilli, S., Roselli, P., Andriulli, A., ... & De Sio, I. (2004). Ultrasound guided fine needle biopsy of early hepatocellular carcinoma complicating liver cirrhosis: a multicentre study. *Gut*, 53(9), 1356-1362.
- Ekstedt, M., Franzén, L. E., Mathiesen, U. L., Thorelius, L., Holmqvist, M., Bodemar, G., & Kechagias, S. (2006). Long-term follow-up of patients with NAFLD and elevated liver enzymes. *Hepatology*, 44(4), 865-873.
- Karamshi, M. (2008). Performing a percutaneous liver biopsy in parenchymal liver diseases. *British Journal of Nursing*, 17(12), 746-752.
- Caturelli, E., Squillante, M. M., Andriulli, A., Siena, D. A., Cellerino, C., De Luca, F., ... & Rapacclni, G. L. (1993). Fine-needle liver biopsy in patients with severely impaired coagulation. *Liver*, 13(5), 270-273.
- Mayo Clinic Staff. (n.d.). Liver disease. Retrieved from: <https://www.mayoclinic.org/diseases-conditions/liver-problems/diagnosis-treatment/drc-20374507>
- McDermott, S., & Gervais, D. A. (2013, March). Radiofrequency ablation of liver tumors. In *Seminars in interventional radiology* (Vol. 30, No. 01, pp. 049-055). Thieme Medical Publishers.
- Venkatesan, A. M., Gervais, D. A., & Mueller, P. R. (2006, March). Percutaneous radiofrequency thermal ablation of primary and metastatic hepatic tumors: current concepts and review of the literature. In *Seminars in interventional radiology* (Vol. 23, No. 01, pp. 073-084). Copyright© 2006 by Thieme

Medical Publishers, Inc., 333 Seventh Avenue, New York, NY 10001, USA.

21. Ryan, M. J., Willatt, J., Majdalany, B. S., Kielar, A. Z., Chong, S., Ruma, J. A., & Pandya, A. (2016). Ablation techniques for primary and metastatic liver tumors. *World journal of hepatology*, *8*(3), 191–199. doi:10.4254/wjh.v8.i3.191
22. Shafi, B. B. B. (2011). Percutaneous radiofrequency ablation of liver tumors. Retrieved from: <https://emedicine.medscape.com/article/1390475-technique>
23. Tatli, S., Tapan, Ü., Morrison, P. R., & Silverman, S. G. (2012). Radiofrequency ablation: technique and clinical applications. *Diagnostic and Interventional Radiology*, *18*(5), 508.
24. Perrault, J., McGill, D. B., Ott, B. J., & Taylor, W. F. (1978). Liver biopsy: complications in 1000 inpatients and outpatients. *Gastroenterology*, *74*(1), 103-106.
25. Cadranel, J. F., Rufat, P., & Degos, F. (2000). Practices of liver biopsy in France: results of a prospective nationwide survey. *Hepatology*, *32*(3), 477-481.
26. de Jong, T. L., Pluymen, L. H., van Gerwen, D. J., Kleinrensink, G. J., Dankelman, J., & van den Dobbelsteen, J. J. (2017). PVA matches human liver in needle-tissue interaction. *Journal of the mechanical behavior of biomedical materials*, *69*, 223-228.

Appendix I: Literature review

Ultrasound-guided liver biopsy specimen adequacy in relation to needle gauge and tip type: a systematic literature review

de Lange, D. (Delft University of Technology)

van den Dobbelsteen, J.J. (Delft University of Technology)

Moelker, A. (Department of Radiology and Nuclear Medicine Erasmus MC Rotterdam)

van de Berg, N.J.P. (Delft University of Technology / Erasmus MC Rotterdam)

Abstract

PURPOSE. The purpose of this systematic review was to compare liver specimen adequacy for histological assessment of percutaneous biopsies in relation to needle gauge and tip type.

METHODS. A comprehensive electronic search was performed, using the Web Of Science and Google Scholar search engines. Eligible studies focussed on at least one of the widely used adequacy criteria: number of portal tracts, total core length (TCL) of the specimen, fragmentation of the specimen, and complication rate. A comparative evaluation was made by classifying these adequacy criteria based on needle gauge and tip type.

RESULTS. A total of 16 eligible studies were included, in which adequacy criteria ranged from 6-11 for number of portal tracts and 15-25 mm for TCL. Results show that decreasing the needle gauge yields a higher number of portal tracts, a longer TCL, and a lower fragmentation rate. No effect of needle gauge on clinical complication rates were evident. Tip type strongly affected specimen adequacy.

CONCLUSION. Optimal needle gauge for obtaining adequate liver specimens varied between 17G-19G. Although more research is needed, needles with opposing bevel tips showed promising results for the selected outcome variables. Overall, developments in needle design, optimal usage, and histological analysis will be crucial, as adequacy criteria were rarely reached in included clinical studies.

KEY WORDS. liver biopsy - fine needle aspiration - core needle biopsy - portal tracts – total core length - fragmentation - complications

1 Introduction

Liver biopsy is required to make a diagnosis, determine the prognosis, and make decisions concerning a treatment plan for hepatic diseases (1, 2). Liver biopsy is one of many diagnostic tools, but is seen as the golden standard and has been a cornerstone in evaluating and managing patients with hepatic diseases (1, 3-7). Hepatitis B (6), hepatitis C (8), hepatocellular carcinoma (HCC) (9), and nonalcoholic fatty liver disease/nonalcoholic steatohepatitis (NAFLD/NASH) (7, 10) are examples of hepatic diseases that depend on liver biopsy for optimal disease treatment and management. Assessing the histology of liver tissue is also of great importance for liver transplantation. It is critical in evaluating the donor liver before it is transplanted into the patient, maximizing donor recipient safety (1, 11).

Percutaneous and endoscopic ultrasound-guided liver biopsy methods can be divided into two techniques: core needle biopsy (CNB) (12) and fine needle aspiration (FNA) (13). FNA typically uses needles with a smaller gauge compared to the needles used in CNB.

Correct diagnosis of hepatic diseases requires a sufficient quality or adequacy of specimens. Established parameters to describe specimen adequacy are the total core length (TCL) and the collected number of portal tracts (14-16). Other parameters that are typically disclosed are incidence rates of specimen fragmentation, as well as complication rates. Complication rates do not describe specimen adequacy, but may affect needle type preference. Overall, specimen adequacy parameters interact. A shorter TCL is often associated with less portal tracts and fragmentation of specimens reduces both TCL and number of portal tracts, decreasing specimen adequacy. Accepted adequacy values differ between studies and range from 15-25 mm and 6-11, for TCL and number of portal tracts respectively (1, 15-20).

The aim of this review is to evaluate the influence of needle gauge and needle tip type on number of portal tracts, total core length (TCL), fragmentation, and complication rates. At present, several publications have reviewed one or more biopsy needle with respect to specimen adequacy. However, a systematic evaluation and comparison of different needle characteristics with respect to specimen adequacy for histological assessment, is still lacking. The reason of this systematic review is to gain insight into the design requirements for an optimal biopsy needle for percutaneous liver biopsy.

2 Materials and Methods

This systematic review was written following the checklist of the PRISMA statement (21).

2.1 Search strategy

A comprehensive electronic search was performed, using the Web Of Science and Google Scholar search engines. The article search was concentrated on search terms – liver, needle, biopsy, fine needle aspiration (FNA), core needle biopsy (CNB). To ensure that relevant publications were not excluded, combinations of subject headings, text word terms and the Boolean operators: AND and OR, were used. The limits imposed were the publishing date; the search term was set from 1998 to 2018, and a language restriction to English. The last search date was August 27th, 2018.

2.2 Study selection

Relevance was determined by analysing the titles and abstracts and through screening the full text of the articles. The reviewer (D. De Lange) screened the titles and abstracts. Full-texts of remaining articles were assessed and subjected to both inclusion and exclusion criteria, see Figure 1.

2.3 Data extraction

Relevant data from the studies that were included in this review were extracted by means of the PICO (population, intervention, comparison, outcome) system, stated in Cochrane Handbook for Systematic Reviews (22). Information extracted included – type of biopsy needle, number of patients involved in the study, type of disease or lesion, number of portal tracts, total core lengths, fragmentations, and complication rates. Complication data focused on biopsy aspects, whereas complications from endoscopic approaches, e.g. during endoscopic ultrasound (EUS) guided biopsy, were excluded.

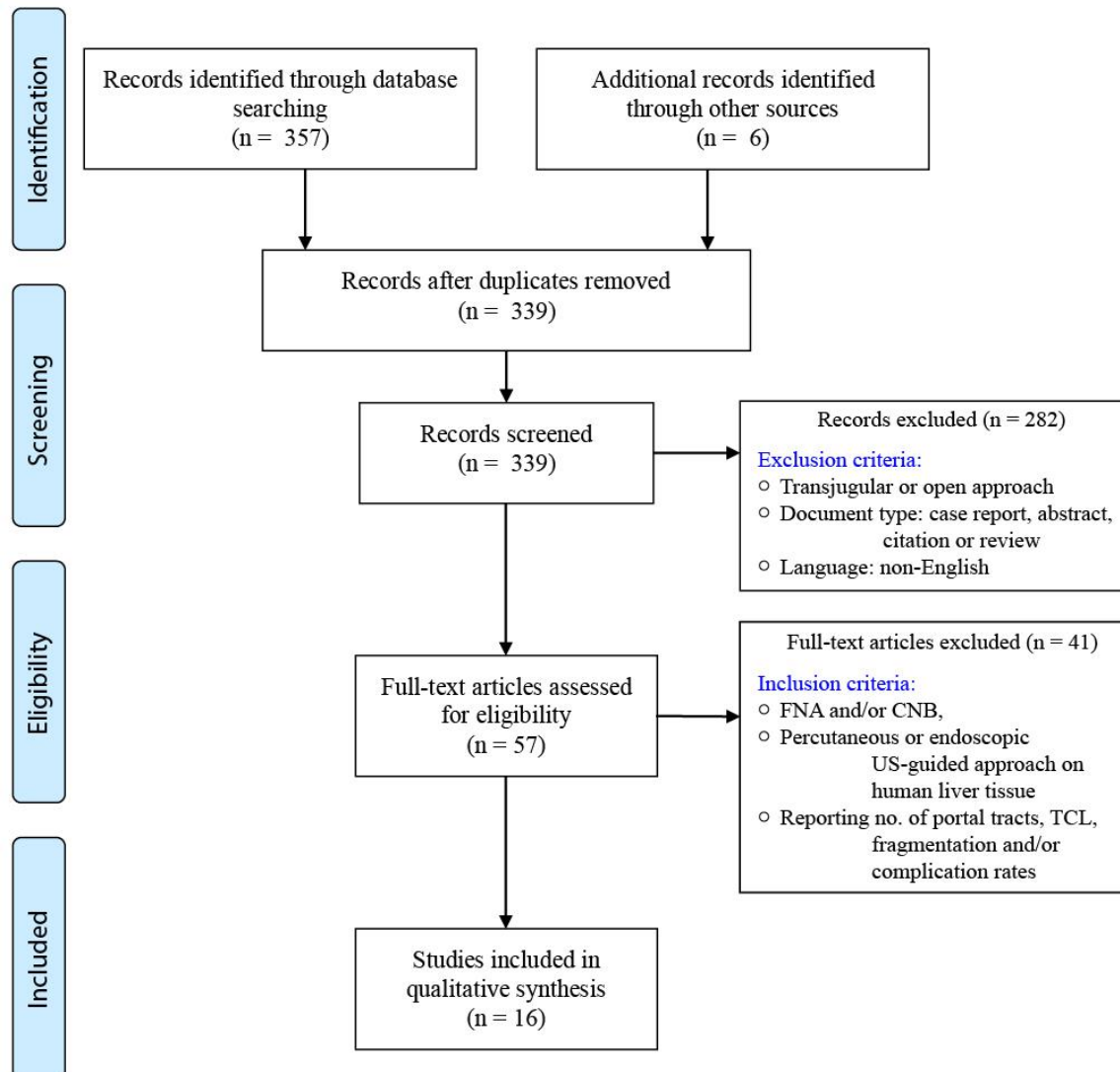


Figure 1. PRISMA Flow diagram of the systematic literature search, indicating inclusion and exclusion criteria and number of articles remaining.

3 Results

3.1 Study characteristics

In total, the literature search resulted in 16 studies, of which 8 studies investigated multiple needles and found results regarding the influence of needles gauge on one or more of the defined outcome variables (23-30), 4 studies investigated multiple needles and found results regarding the influence of needles' tip design on the outcome variables (24, 31-33), and 5 studies investigated a single needle on the outcome variables (14, 17, 18, 34, 35). A total of fourteen different needles was found within these studies and details of the needle and study characteristics are presented in Table 1.

3.2 Effects of needle gauge

In this review, 8 of the 16 studies investigated multiple needles in order to determine the influence of needle gauge on the number of portal tracts obtained, the total core length (TCL) of the specimen, fragmentation of the specimen and/or complication rate (23-30).

3.2.1 Number of portal tracts

The relationship between needle gauge and the number of portal tracts obtained was investigated in 4 of the 8 studies (23-26). Number of portal tracts is defined as the number of complete portal tracts.

All four studies that investigated the relationship between needle gauge and number of portal tracts showed a significantly larger amount of portal tracts for needles with a smaller needle gauge (larger diameter), compared to needles with a larger needle gauge (smaller diameter). However, one study found contrasting results as well. An overview of this data is given in figure 2.

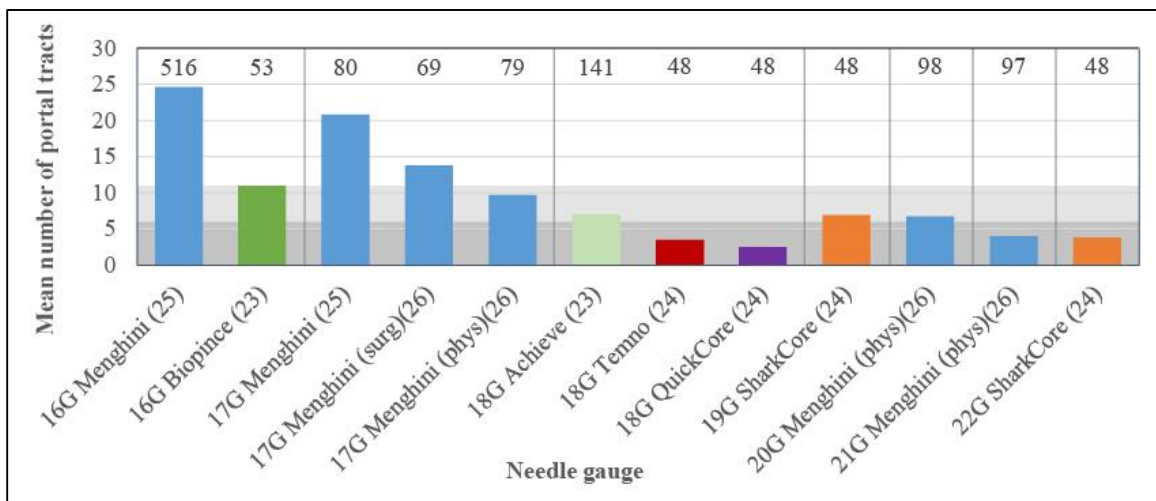


Figure 2: Comparison of mean number of portal tracts by needle gauge. Equal needle types are indicated by equal colors. The number of biopsies performed with a particular needle are depicted above the bars. The light grey and dark grey areas indicate the upper and lower bounds of the defined range for adequate numbers of portal tracts. Surg means biopsies were performed by surgeons, whereas phys means biopsies were performed by physicians.

Of the ten different needle types (varying in needle gauge or tip type) in figure 2, the *mean* number of portal tracts obtained was below the lower bound of adequacy for four needles, within the arguably adequate range for three needles, and above the upper bound for three needles (16G Menghini, 17G Menghini and 16G Biopince). Here, we considered a number-of-biopsies-weighted average of the collective data for the 17G Menghini needle.

Hall et al. (23) found the mean number of portal tracts obtained with the 16G Biopince needle to be significantly higher than the 18G Achieve needle. The mean number of portal tracts \pm standard deviation, was 11 ± 4.2 and 7 ± 3.4 for Biopince and Achieve needles, respectively ($p < 0.0005$). Schulman et al (24) also found that the mean number of portal tracts obtained with the 19G SharkCore needle was significantly higher compared to the smaller 22G SharkCore needle ($p < 0.001$). In contrast, the 19G SharkCore needle obtained a higher number of portal tracts compared to the 18G QuickCore and 18G Temno needles ($p < 0.001$). The mean number of portal tracts was 6.2, 3.8, 2.5, and 3.5, respectively. Sporea et al. (25) found a significantly larger amount of portal tracts obtained with the 16G Menghini needle compared to the 17G Menghini needle ($p = 0.003$). The mean number of portal tracts \pm standard deviation was 24.6 ± 10.6 and 20.8 ± 8.6 , respectively. Finally, Röcken et al. (26) compared biopsies by surgeons and physicians and found the mean number of portal tracts obtained with 17G Menghini (phys) and 17G Menghini (surg) needles to be significantly higher compared to 20G and 21G Menghini (phys) needles ($p < 0.05$). The mean number of portal tracts obtained with the 20G (phys) needle was also significantly higher compared to the 21G (phys) needle ($p < 0.05$). The mean number of portal tracts \pm standard deviation, was 13.8 ± 6.5 in the case of the 17G (surg) needle, 9.7 ± 5.9 in the case of the 17G (phys) needle, 6.7 ± 4.4 in the case of the 20G (phys) needle, and 4.0 ± 3.1 in the case of the 21G (phys) needle.

Appendix I

Table 1: Needle types and research methodology characteristics of included outcome variables in this literature review.

Needle Type	Method	Needle gauge	Type	Company	Number of biopsies	Median number of passes	Reason biopsy	Biopsy site	Ref.
Achieve	CNB	18	end-cut full core	Argon Medical	141	-	Parenchymal liver disease	-	(23)
Biomol	FNA/CNB	21	menghini type semi-automatic biopsy device	Hospital Service	149	1	Diffuse liver disease	-	(29)
Biopince	CNB	16	Tri-axial core cut and capture system	Care-fusion	53	-	Parenchymal liver disease	-	(23)
Echotip	EUS-CNB	19	Bevel tip	Wilson-Cook Medical Inc.	22	2	Abnormal liver tests	Left lobe	(34)
Expect	EUS-FNA	19	Deep needle bevel tip	Boston Scientific	48	1-3 with FT	-	Nondiseased liver tissue	(24)
		19	Deep needle bevel tip Slimline	Boston Scientific	12	1 with 3,6,9 BFM and FT	-	Left, right lobe	(31)
		19	Deep needle bevel tip	Boston Scientific	10	3 with 3 BFM per pass	Abnormal liver functions	Left lobe	(14)
EZ Shot	EUS-FNA	19	Menghini tip	Olympus	12	1 with 3,6,9 BFM and FT	-	Left, right lobe	(31)
FNAC	FNA/CNB	21	Aspirating and cutting	HAKKO	48	1 with 3-5 BFM	Malignant tumor	-	(28)
Hepa-cut	CNB	18	Menghini	Sterylab	149	1	Diffuse liver disease	-	(29)
Menghini	FNA	16,17	Hepafix	Braun Melsungen AG	516, 80	2	Chronic diffuse liver diseases	-	(25)
		17,20,21	Menghini tip	-	148, 98, 97	1		-	(26)
ProCore	EUS-CNB	19	Echo Menghini Tip HD	-	48	1-3 with FT	-	Nondiseased liver tissue	(24)
		19	Echo Menghini Tip	Cook Medical Inc.	12	1 with 3,6,9 BFM and FT	-	Left, right lobe	(31)
		19	Menghinit tip	Cook Medical Inc.	30	2	Parenchymal liver disease	Left lobe	(32)
		19	Menghini tip	Wilson-Cook Medical Inc.	5	2	-	-	(33)
		18	bevel tip and rapid-firing mechanism	Cook Medical Inc.	48	1-3 with FT	-	Nondiseased liver tissue	(24)
QuickCore	EUS-CNB	19	bevel tip and rapid-firing mechanism	Cook Medical Inc.	45	3	Parenchymal liver disease	Left lobe	(32)
		19	bevel tip and rapid-firing mechanism	Cook Medical Inc.	8	2	Suspected tumor or parenchymal diseases	-	(33)
		19	bevel tip and rapid-firing mechanism	Cook Medical Inc.	9	2	Hepatic parenchymal disease	Left lobe	(17)
		19	bevel tip and rapid-firing mechanism	Cook-Endoscopy	21	3	Parenchymal liver disease	Left lobe	(18)
		19,22	Opposing bevel tip	Medtronic	48	1-3 with FT	-	Nondiseased liver tissue	(24)
SharkCore	EUS-CNB	19	1-pass 1 actuation wet suction technique, opposing bevel tip	Medtronic	330	1 for 7 cm deep	Abnormal liver functions	Left, right lobe	(35)
		19	Opposing bevel tip	Covidien	12	1 with 3,6,9 BFM and FT	-	Left, right lobe	(31)
Temno	CNB	18,20	spring loaded semi-automated	Cardinal Health	722, 49	2/3	Parenchymal liver disease	Left, right lobe	(27)
		18	spring loaded semi-automated, coaxial	Care-fusion	48	1-3 with FT	-	Nondiseased liver tissue	(24)
Tru-cut	CNB	18	Bevel tip and side notch	Cook Medical	46	1 with 3-5 BFM	Malignant tumor	-	(28)

Notes. CNB: Core Needle Biopsy, BFM: Back-and-Forward Motions, EUS: Endoscopic Ultrasound, FNA: Fine Needle Aspiration, FNAC: Fine Needle Aspirating and Cutting, FT: Fanning Technique

3.2.2 Total core length

The relationship between needle gauge and the TCL of specimens was investigated in 5 of the 8 studies (23, 26-29).

The relationship between needle gauge and TCL showed a significantly higher mean TCL for needles with a smaller needle gauge (larger diameter) compared to needles with a larger needle gauge (smaller diameter) in 4 out of 5 studies. One study found contrasting results, which possibly resulted from a second categorical variable of interest, the end-user of the biopsy needle. One study did not find differences between needle gauge and TCL of the specimen. Mean TCLs of needles per study are shown in figure 3. Bars with the same colour contain data of the same type of needles. Number of biopsies performed are depicted above the bars. The light grey and dark grey areas indicate the upper and lower bounds for the defined adequacy range for TCL.

A total of nine different needle types (varying in needle gauge or tip type) are shown in figure 3. The *mean* TCL obtained with these needles was below the lower bound of adequacy for two needles, within the arguably adequate range for five needles, and above the upper bound for two needles, respectively the 17G and 20G Menghini needles.

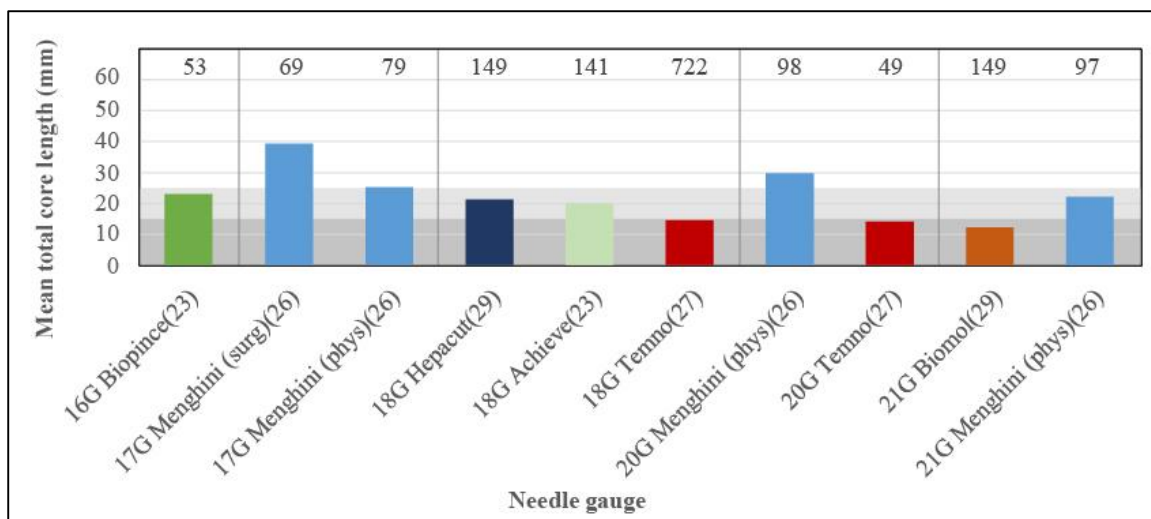


Figure 3: Comparison of mean total core length by needle gauge. Equal needle types are indicated by equal colors. The number of biopsies performed with a particular needle are depicted above the bars. The light grey and dark grey areas indicate the upper and lower bounds of the defined range for adequate total core lengths. Surg means biopsies were performed by surgeons, whereas phys means biopsies were performed by physicians.

Hall et al. (23) demonstrated a significantly higher mean TCL obtained with the 16G Biopince needle compared to the 18G Achieve needle ($P = 0.0005$). Mean TCLs were $23 \text{ mm} \pm 4.1 \text{ mm}$ and $20 \text{ mm} \pm 6.8 \text{ mm}$, respectively. A retrospective study by Vijayaraghavan et al. (27) found no difference between the mean TCL of 18G and 20G Temno needles ($p = 0.531$). The mean TCLs \pm standard deviations were $14.4 \text{ mm} \pm 3.7 \text{ mm}$ and $14.1 \text{ mm} \pm 3.4 \text{ mm}$, respectively. Li et al. (28) presented the number of obtained samples per needle with a $\text{TCL} > 5 \text{ mm}$. A significantly larger amount of liver biopsies with a $\text{TCL} > 5 \text{ mm}$ ($p = 0.002$) was obtained with the 18G Trucut needle (82.6%) compared to the 21G FNAC needle (52.1%). Mean values for the TCL were not given within this study. Brunetti et al. (29) found a significantly higher mean TCL for liver

biopsies obtained with the 18G Hepa-cut needle compared to the 21G Biomol needle ($p < 0.001$). The TCL was 21.2 mm and 12.2 mm for the 18G and 21G needle, respectively. Röcken et al. (26) found a significantly higher mean TCL for the 17G Menghini (surg) needle compared to the 17G Menghini (phys) and, 20G and 21G Menghini (phys) needles. The 17G (phys) needle had a significantly larger mean TCL compared to the 21G (phys) needle ($p < 0.05$). However, the 20G (phys) needle had a significantly higher mean TCL compared to the larger 17G (phys) needle ($p < 0.05$). The mean TCL \pm standard deviation was 39.4 mm \pm 17.4 mm in the case of the 17G (surg) needle, 25.3 mm \pm 11.3 mm, in the case of the 17G (phys) needle, 29.8 mm \pm 12.9 mm in the case of the 20G (phys) needle and 22.1 mm \pm 12.7 mm in the case of the 21G (phys) needle.

3.2.3 Fragmentation

The effect of needle gauge on fragmentation of biopsy specimens was investigated in 4 of the 8 studies (23, 24, 26, 29).

A lower percentage of fragmentation for needles with a smaller gauge (larger diameter) compared to needles with a larger gauge (smaller diameter) was found in 3 of the 4 included studies. One study did not find a relation between needle gauge and fragmentation of biopsy specimens. An overview of the percentages of fragmentation for the different needle types is plotted against needle gauge in figure 4.

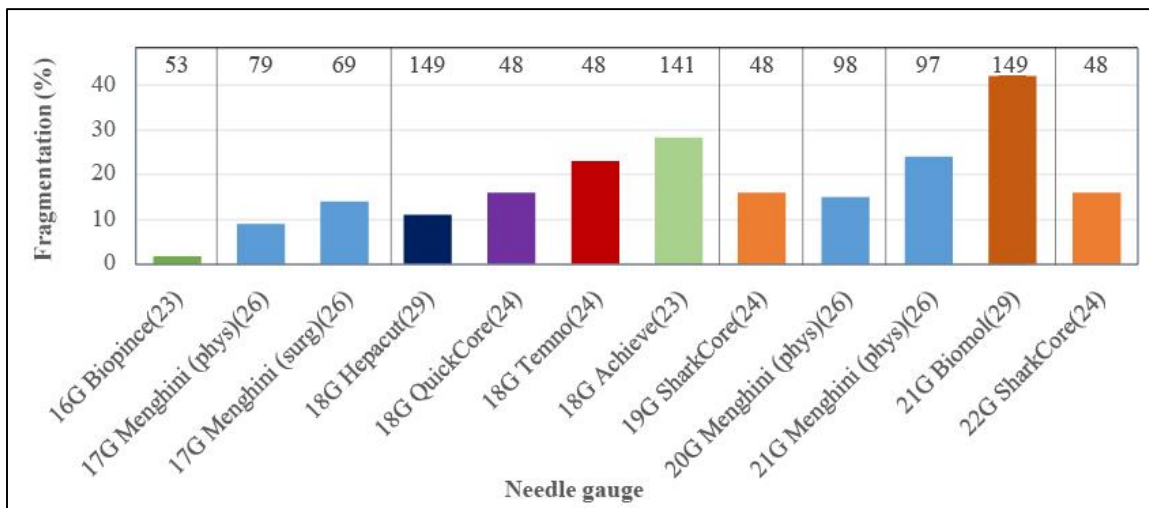


Figure 4: Comparison of fragmentation percentages by needle gauge. Equal needle types are indicated by equal colors and the number of biopsies performed with that particular needle are depicted above the bars.

Hall et al. (23) found a significant lower percentage of fragmented biopsy samples for the 16G Biopince needle compared to the 18G Achieve needle ($p = 0.0001$), with respectively 1.8% and 28.3% of fragmented samples. A significantly lower percentage of fragmentation was also found for the 18G Hepa-cut needle compared to the 21G Biomol needle in Brunetti et al. (29). The 18G needle yielded fragmented specimens in 11% of the cases, while 42% was fragmented in the cases where the 21G needle was used. Röcken et al. (26) found a significantly lower percentage of fragmentation in the samples obtained with the 17G Menghini needle, compared to the 21G Menghini needle (9% and 24%, $p < 0.01$). The 20G Menghini needle obtained fragmented samples in 15% of the cases, however no difference was found between the 17G and 20G needles or the 20G and 21G

needles. Schulman et al (24) found no difference in the incidence of sampling either fragments or pieces (see article for definitions), when comparing 19G SharkCore (16%), 22G SharkCore (16%), 18G QuickCore (16%) and 18G Temno (23%) needles.

3.2.4 Complication rate

The relationship between needle gauge and the rate of complications occurring during or after procedures was investigated in 5 of the 8 studies (23, 25, 27, 28, 30).

No relations between needle gauge and complication rates were reported in 4 of the 5 studies. A significantly higher incidence rate of pain for patients that underwent liver biopsy with a needle with a smaller needle gauge (larger diameter), compared to patients that underwent liver biopsy with a needle with a larger needle gauge (smaller diameter) was found in 1 of the 5 studies.

Hall et al. (23) reported minor complications, pain being the most frequently encountered, in 27 patients using the 16G Biopince needle (53 included biopsies) and 14 patients using the 18G Achieve needle (141 included biopsies). They concluded both needles had a similar risk on complications. Sporea et al. (25) reported no complications or fatalities as a result of the liver biopsies using 16G and 17G Menghini needles. Vijayaraghavan et al (27) performed a study with Temno needles and reported that 13 out of the 771 cases experienced moderate to severe pain, 6 cases experienced clinically severe haemorrhage, 5 cases major bleeds and 1 case of mortality. No relations with needle gauge was seen in the study of Vijayaraghavan et al ($p > 0.343$). Similarly, Karacaer et al (30) did not find relations between the development or presence of severe pain and the diameter of the needle that was used to obtain a biopsy specimen ($p = 0.322$). However, severe pain developed most frequently after using the 16G needles in the study of Karacaer et al (30), regardless of the method that was used ($p = 0.001$). Contrasting results were found by Li et al (28), presenting a higher incidence rate of pain (VAS - Visual Analogue Scale ≥ 1) in patients treated with the 18G Trucut needle, compared to the 21G FNAC needle ($p < 0.001$). Pain (VAS ≥ 1) was observed in 78.3% and 22.9% of patients, respectively. The average VAS score was also significantly higher for the 18G group compared to the 21G group ($p < 0.001$).

3.3 Effects of needle tip type

To limit confounding effects of needle gauge, the tip type comparison focuses on 19G needles, which was the most commonly encountered size in included studies. Although this resulted from the popularity of 19G needles in EUS LB procedures, it is assumed that the effect of tip type is generalizable to different clinical approaches.

Two or more 19G needles with different tip types and presented data on number of portal tracts, TCL of the specimen or fragmentation rate were investigated in 4 out of 16 studies (24, 31-33). Number of needle passes is discussed if this was fixed before performing the liver biopsies. The included tip types are presented in figure 5. Additionally, 5 of the 16 studies assessed a single 19G needle regarding the number of portal tracts obtained, the TCL of the specimen, or fragmentation of the specimen (14, 17, 18, 34, 35). Results of these studies are included in figures 6-8.

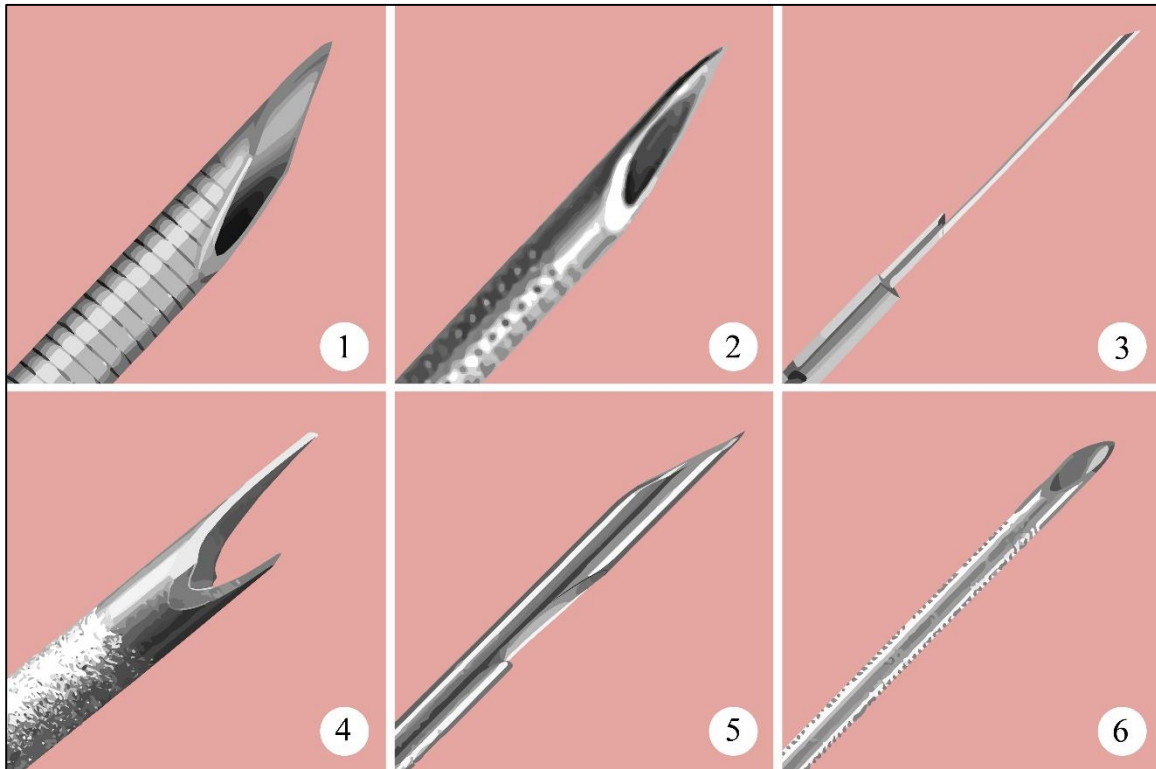


Figure 5: The different needle tip types: 1. Expect needle with deep needle bevel tip, 2. EZ Shot needle with Menghini tip, 3. Quickcore needle with bevel tip and rapid-firing mechanism, 4. Sharkcore needle with opposing bevel tip, 5. Procore needle with Menghini bevel tip and core trap side notch, 6. Echotip needle with bevel tip.

3.3.1 Number of portal tracts

All 4 studies that compared 19G needles, showed results on the influence of needle tip type on the number of complete portal tracts obtained (24, 31-33). The number of portal tracts is plotted for the different needle types in figure 6.

Although overlap in the included 19G biopsy needles in the 4 comparative studies was limited, no directly contrasting results were seen when ranking performance in terms of obtained number of portal tracts. The SharkCore needle performed best (included in 2 studies), followed by the EZ Shot needle (1 study), Expect and ProCore needles (2 studies), and the QuickCore needle (2 studies).

Of the six tip types included in this comparison, one tip type (SharkCore), and in one study only, the upper bound for number of portal tracts was exceeded. In two other studies, this same needle remained within the arguably adequate range with an average (number-of-biopsies-weighted) of 6.7 portal tracts. One other tip type (Echotip) reached a median number of portal tracts within this range. The obtained number of portal tracts of the remaining four needles largely remained below the lower bound of adequacy, with 4.3 and 3.3 portal tracts (number-of-biopsy-weighted) for the ProCore and Expect needles, respectively.

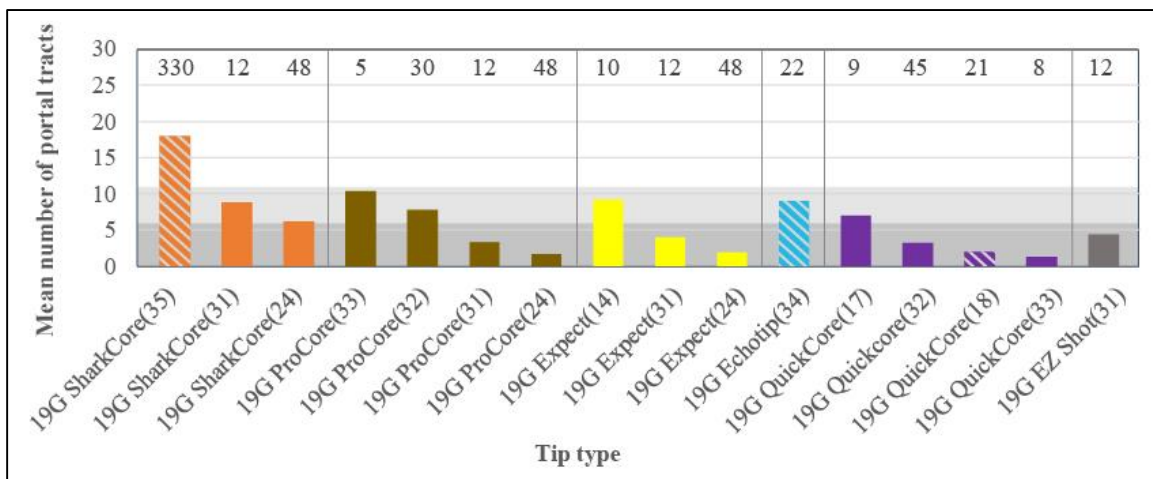


Figure 6: Comparison of number of portal tracts by needle type. Equal needle types are indicated by equal colors. The number of biopsies performed with a particular needle is depicted above the bar. Solid filled bars indicate reported mean values, shaded bars indicate reported median values. The light grey and dark grey areas indicate the upper and lower bounds of the defined range for adequate numbers of portal tracts. Needle types are plotted from highest to lowest number of portal tracts and data from the same needle type is plotted next to each other.

Schulman et al. (24) found a significantly increased mean number of portal tracts for the 19G SharkCore needle compared to the ProCore and the Expect needle ($p < 0.001$). Mean number of portal tracts was 6.2, 1.7 and 1.9, respectively. No difference was found between the ProCore and the Expect needle ($p = 0.769$). A significantly higher mean number of portal tracts was also obtained in a single pass for the SharkCore needle (4.1) compared to the ProCore (1.3) and Expect (0.7) needles ($p = 0.002$; $p < 0.001$). Lee et al. (31) tested four needles, of which three were identical to the ones tested by Schulman et al. (24). They also found a significantly higher overall mean number of portal tracts for the SharkCore needle compared to the other three needles ($p < 0.01$). The overall mean number of portal tracts were 8.8, 4.0, 3.3, and 4.4 for the SharkCore, Expect, ProCore, and EZ Shot, respectively. The number of BFM did not have a significant relationship with the mean number of portal tracts ($p \leq 0.17$). Sey et al. (32) Found a significant higher mean number of portal tracts with a ProCore needle compared to a QuickCore needle ($p = 0.0003$). The ProCore needle achieved a mean number of portal tracts \pm standard deviation of 7.8 ± 6.4 , whereas 3.2 ± 3.8 was achieved for the QuickCore needle. A different study with the same ProCore and QuickCore needle was performed by DeWitt et al. (33). A significant higher number of portal tracts was achieved with the ProCore needle compared to the QuickCore needle ($p = 0.0004$). The mean number of portal tracts \pm standard deviation was 10.4 ± 4.7 and 1.3 ± 1.9 , respectively.

3.3.2 Total core length

The influence of needle tip type on TCL of the specimen was presented in 3 of the 4 studies (31-33). The TCL is plotted for the different needle types in figure 7. In 2 out of 3 studies, a higher TCL for the ProCore needle, compared to the QuickCore needle, was found. In one study, no relations between TCL and tip type were apparent.

Of the six included tip types, four resulted in adequate values for TCL (SharkCore, ProCore, EZ Shot and Echotip), one resulted in arguably adequate values for TCL and one remained below the lower bound of adequacy.

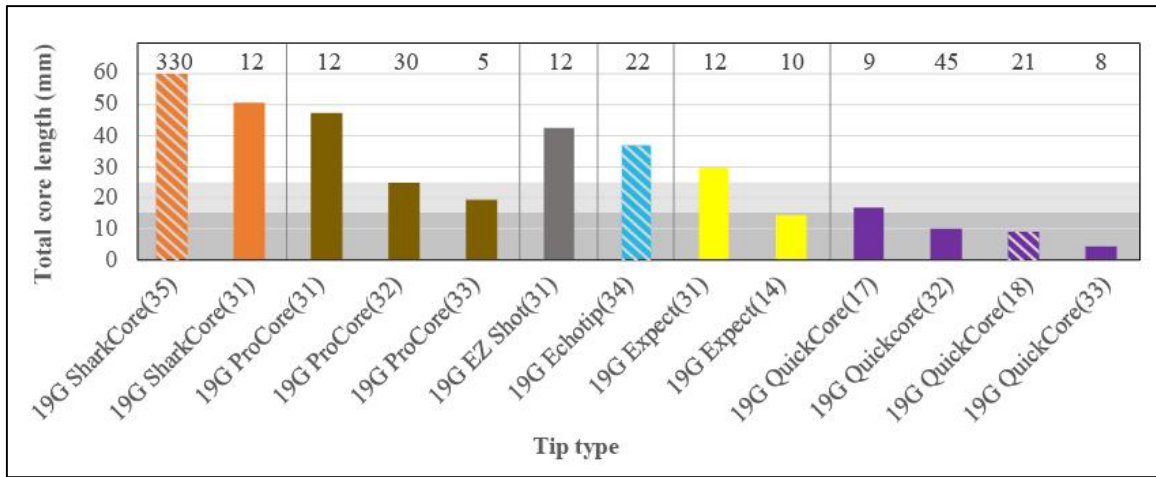


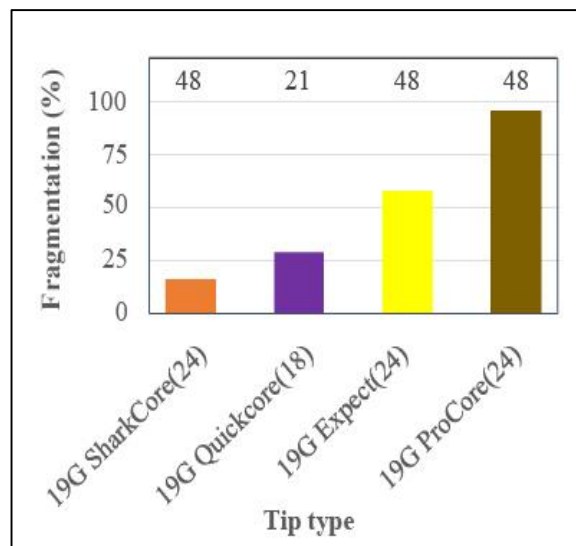
Figure 7: Comparison of total core length of the specimen by needle type. Equal needle types are indicated by equal colors. The number of biopsies performed with a particular needle are depicted above the bars. Solid filled bars indicate reported mean values, shaded bars indicate reported median values. The light grey and dark grey areas indicate the upper and lower bounds of the defined range for adequate total core lengths. Needles types are plotted from highest to lowest mean TCL and data from the same needle type is plotted next to each other.

Lee et al. (31) found no difference in TCL when comparing SharkCore, ProCore, EZ Shot and Expect needles. The obtained mean TCL of these needles was respectively 50.7 mm, 47.3 mm, 42.6 mm and 29.8 mm. Sey et al. (32) found a significantly higher mean TCL for the ProCore needle compared to the QuickCore needle ($p < 0.0001$). The mean TCL \pm standard deviation was 24.8 mm \pm 14.9 mm and 10.1 mm \pm 7.0 mm, respectively. DeWitt et al. (33) also found a significantly higher TCL for the 19G ProCore needle compared to the 19G QuickCore needle ($p = 0.001$). The mean TCL \pm standard deviation was 19.4 \pm 14.1 and 4.3 \pm 4.5, respectively.

3.3.3 Fragmentation

One of the included studies investigated the influence of needle tip type on the percentage of fragmentation in specimens (24). Schulman et al (24) encountered fragmentation in 16%, 58% and 96% of specimens after use of 19G SharkCore, Expect and ProCore needles, respectively. Fragmentation per needle type is shown in Figure 8.

Figure 8: Comparison of fragmentation percentages by needle type. The number of biopsies performed with a particular needle are depicted above the bars.



4 Discussion

The aim of this review is to evaluate the effect of needle gauge and tip type on number of portal tracts, TCL, fragmentation and complication rates. To reduce interacting effects, the review was divided in two sections, where tip type comparisons solely focused on 19G needles. Simultaneously, this resulted in an EUS LB focused section, as 19G needles are commonly used in this setting. It is assumed that relative effects of tip types are generalizable to different clinical approaches.

The results show an overall higher number of portal tracts, a longer TCL, and a lower fragmentation rate for needles with a larger diameter. The effect of needle gauge on complication rate was disclosed in a limited number of studies. No effects were reported in 4 studies, and a slightly higher complication rate was reported in 1 study, for needles with a smaller gauge. The results further show large effects of tip types. SharkCore and Echotip needles performed best in terms of TCL and number of portal tracts obtained. Menghini needles and other types included in the needle gauge comparison, of which comparative 19G needle data was missing, may provide adequate alternatives.

When considering biopsy adequacy criteria presented in literature, 17G needles should be used to collect sufficient portal tracts, while limiting fragmentation. However, some effective tip types may lower these demands, e.g. 19G SharkCore needle. When considering adequacy criteria for TCL, tip type appears to have a much stronger effect than needle gauge. Currently, SharkCore, ProCore, EZ Shot and Echotip needles seem to perform sufficiently well. Fragmentation seems to depend strongly on both needle gauge and tip type. SharkCore and QuickCore needles had the lowest fragmentation rates.

Accepted values in literature for biopsy adequacy, in terms of number of portal tracts, ranges between 6 and 11, i.e. the arguably adequate range. Of the collective 28 *mean* or *median* number of portal tracts reported, only 5 (18%) exceeded the upper bound of this range, 11 (39%) were within the range, and 12 (43%) remained below the lower bound. For TCL, the arguably adequate range was 15-25 mm. Of the collective 23 *mean* or *median* TCL values reported, 10 (43%) exceeded, 6 (26%) were within, and 7 (30%) remained below this range. Since it is desirable to have all or most of biopsied specimens to be of adequate quality, instead of means or medians, progressions in biopsy needle design, optimal instrument usage, and histological specimen analysis will be of great value.

Reported outcome variables are affected by many factors, which may not be equally well controlled in all of the included studies. Vijayaraghavan et al (19) showed that the TCL of a specimen obtained with 1 or 2 passes is significantly longer than the TCL of a specimen obtained with 3 or more passes. The number of passes for obtaining a liver biopsy was fixed in some studies, while in other studies the number of passes relied on visual inspection of TCL by the surgeon or physician. Some studies also used a fanning technique for each pass, while other studies did not describe or use such a technique. Two of the included studies were performed *ex-vivo*, while 14 were performed *in-vivo*. In addition, Sporea et al (36) showed that senior (performed > 100 liver biopsies) operators obtained a significantly higher TCL of specimens and a significantly higher number of portal tracts, compared to junior (performed < 100 liver biopsies) operators ($p < 0.001$). Better specimens were obtained by surgeons or physicians with more years of expertise or a higher number of liver biopsies performed. The clinical approach (percutaneous or endoscopic guided) was also an important factor in presented results. This is visible when comparing the bars of the two sections in this review (needle gauge and tip type). Finally, hepatic

diseases, severity and distributions differed between studies and affected outcome variables (16, 26). Much more data on biopsy needle performance will be required to properly differentiate the impact of these factors and optimize devices and techniques.

In conclusion, a higher number of portal tracts, longer TCL of the specimen, and lower fragmentation rate were associated with larger diameter needles. When comparing results to biopsy adequacy requirements defined in literature, the use of needle diameters between 17G and 19G is advised. Tip type seemed to strongly affect specimen adequacy. Although more research is needed, needles with an opposing bevel tip design appeared to be particularly promising when comparing number of portal tracts, TCL of the specimen and fragmentation rates. When considering the softest adequacy criteria used in literature, 43% of mean/median number of portal tracts and 30% of mean/median TCLs reported, were inadequate. Since it is desirable to have all or most of biopsied specimens to be of adequate quality, instead of means or medians, progressions in biopsy needle design, optimal instrument usage, and histological specimen analysis will be of great value.

6 Abbreviations

BFM	back-and-forward motions
CNB	core needle biopsy
EUS	endoscopic ultrasound
FNA	fine needle aspiration
FNAC	fine needle aspirating and cutting
FT	fanning technique
G	gauge
HCC	hepatocellular carcinoma
NAFLD	nonalcoholic fatty liver disease
NASH	nonalcoholic steatohepatitis
TCL	total core length
US	ultrasound
VAS	visual analogue scale

7 References

1. Rockey DC, Caldwell SH, Goodman ZD, Nelson RC, Smith AD. Liver biopsy. *Hepatology*. 2009;49(3):1017-44.
2. Sherman M, Bruix J. Biopsy for liver cancer: How to balance research needs with evidence-based clinical practice. *Hepatology*. 2015;61(2):433-6.
3. Campbell M, Reddy K. The evolving role of liver biopsy. *Aliment Pharm Ther*. 2004;20(3):249-59.
4. Pineda JJ, Diehl DL, Miao CL, Johal AS, Khara HS, Bhanushali A, et al. EUS-guided liver biopsy provides diagnostic samples comparable with those via the percutaneous or transjugular route. *Gastrointest Endosc*. 2016;83(2):360-5.
5. Lefkowitz JH. *Scheuer's Liver Biopsy Interpretation E-Book*: Elsevier Health Sciences; 2015.
6. Mani H, Kleiner DE. Liver biopsy findings in chronic hepatitis B. *Hepatology*. 2009;49(S5):S61-S71.
7. Brunt EM, editor *Nonalcoholic steatohepatitis: definition and pathology. Seminars in liver disease*; 2001: Copyright© 2001 by Thieme Medical Publishers, Inc., 333 Seventh Avenue, New York, NY 10017.
8. Dienstag JL. The role of liver biopsy in chronic hepatitis C. *Hepatology*. 2002;36(S1):S152-S60.
9. Caturelli E, Solmi L, Anti M, Fusilli S, Roselli P, Andriulli A, et al. Ultrasound guided fine needle biopsy of early hepatocellular carcinoma complicating liver cirrhosis: a multicentre study. *Gut*. 2004;53(9):1356-62.
10. Ekstedt M, Franzén LE, Mathiesen UL, Thorelius L, Holmqvist M, Bodemar G, et al. Long-term follow-up of patients with NAFLD and elevated liver enzymes. *Hepatology*. 2006;44(4):865-73.
11. Ryan CK, Johnson LA, Germin BI, Marcos A. One hundred consecutive hepatic biopsies in the workup of living donors for right lobe liver transplantation. *Liver Transplant*. 2002;8(12):1114-22.
12. Philpotts LE, Hooley RJ, Lee CH. Comparison of automated versus vacuum-assisted biopsy methods for sonographically guided core biopsy of the breast. *Am J Roentgenol*. 2003;180(2):347-51.
13. Amedee RG, Dhurandhar NR. Fine-needle aspiration biopsy. *The Laryngoscope*. 2001;111(9):1551-7.
14. Gor N, Salem SB, Jakate S, Patel R, Shah N, Patil A. Histological adequacy of EUS-guided liver biopsy when using a 19-gauge non-Tru-Cut FNA needle. *Gastrointest Endosc*. 2014;79(1):170-2.
15. Bravo AA, Sheth SG, Chopra S. Liver biopsy. *New England Journal of Medicine*. 2001;344(7):495-500.
16. Cholongitas E, Senzolo M, Standish R, Marelli L, Quaglia A, Patch D, et al. A systematic review of the quality of liver biopsy specimens. *Am J Clin Pathol*. 2006;125(5):710-21.
17. Gleeson FC, Clayton AC, Zhang L, Clain JE, Gores GJ, Rajan E, et al. Adequacy of endoscopic ultrasound core needle biopsy specimen of nonmalignant hepatic parenchymal disease. *Clin Gastroenterol H*. 2008;6(12):1437-40.

18. DeWitt J, McGreevy K, Cummings O, Sherman S, LeBlanc JK, McHenry L, et al. Initial experience with EUS-guided Tru-cut biopsy of benign liver disease. *Gastrointest Endosc.* 2009;69(3):535-42.
19. Colloredo G, Guido M, Sonzogni A, Leandro G. Impact of liver biopsy size on histological evaluation of chronic viral hepatitis: the smaller the sample, the milder the disease. *J Hepatol.* 2003;39(2):239-44.
20. Bedossa P, Dargère D, Paradis V. Sampling variability of liver fibrosis in chronic hepatitis C. *Hepatology.* 2003;38(6):1449-57.
21. Moher D, Liberati A, Tetzlaff J, Altman DG, Group P. Preferred reporting items for systematic reviews and meta-analyses: the PRISMA statement. *PLoS medicine.* 2009;6(7):e1000097.
22. Higgins JP, Green S. *Cochrane handbook for systematic reviews of interventions.* 2008.
23. Hall TC, Deakin C, Atwal GSS, Singh RK. Adequacy of percutaneous non-targeted liver biopsy under real-time ultrasound guidance when comparing the Biopince (TM) and Achieve (TM) biopsy needle. *Brit J Radiol.* 2017;90(1080).
24. Schulman AR, Thompson CC, Odze R, Chan WW, Ryou M. Optimizing EUS-guided liver biopsy sampling: comprehensive assessment of needle types and tissue acquisition techniques. *Gastrointest Endosc.* 2017;85(2):419-26.
25. Sporea I, Gherhardt D, Popescu A, Sirli R, Cornianu M, Herman D, et al. Does the size of the needle influence the number of portal tracts obtained through percutaneous liver biopsy? *Ann Hepatol.* 2015;11(5):691-5.
26. Röcken C, Meier H, Klauck S, Wolff S, Malferttheiner P, Roessner A. Large-needle biopsy versus thin-needle biopsy in diagnostic pathology of liver diseases. *Liver.* 2001;21(6):391-7.
27. Vijayaraghavan GR, Vedantham S, Rangan V, Karam A, Zheng L, Roychowdhury A, et al. Effect of needle gauge and lobe laterality on parenchymal liver biopsy outcome: a retrospective analysis. *Abdom Imaging.* 2015;40(5):1223-9.
28. Li G-P, Gong G-Q, Wang X-L, Chen Y, Cheng J-M, Li C-Y. Fine needle aspirating and cutting is superior to Tru-cut core needle in liver biopsy. *Hepatob Pancreat Dis.* 2013;12(5):508-11.
29. Brunetti E, Silini E, Pistorio A, Cavallero A, Marangio A, Bruno R, et al. Coarse vs. fine needle aspiration biopsy for the assessment of diffuse liver disease from hepatitis C virus-related chronic hepatitis. *J Hepatol.* 2004;40(3):501-6.
30. Karacaer Z, Yilmaz Karadag F, Durmus G, Cicek H, Parlak E, Ari A, et al. Percutaneous Liver Needle Biopsy Methods Can Be Safe and Effective in Patients with Viral Hepatitis. *Viral Hepat Derg.* 2017;23(3):65-70.
31. Lee WJJ, Uradomo L, Zhang Y, Twaddell W, Darwin P. Comparison of the Diagnostic Yield of EUS Needles for Liver Biopsy: Ex-Vivo Study. *Gastrointest Endosc.* 2016;83(5):Ab516-Ab.
32. Sey MSL, Al-Haddad M, Imperiale TF, McGreevy K, Lin JM, DeWitt JM. EUS-guided liver biopsy for parenchymal disease: a comparison of diagnostic yield between two core biopsy needles. *Gastrointest Endosc.* 2016;83(2):347-52.
33. DeWitt J, Cho C-M, Lin J, Al-Haddad M, Canto MI, Salamone A, et al. Comparison of EUS-guided tissue acquisition using two different 19-gauge core biopsy needles: a

multicenter, prospective, randomized, and blinded study. *Endoscopy international open*. 2015;3(05):E471-E8.

34. Stavropoulos SN, Im GY, Jlayer Z, Harris MD, Pitea TC, Turi GK, et al. High yield of same-session EUS-guided liver biopsy by 19-gauge FNA needle in patients undergoing EUS to exclude biliary obstruction. *Gastrointest Endosc*. 2012;75(2):310-8.

35. Nieto J, Khaleel H, Challita Y, Jimenez M, Baron TH, Walters L, et al. EUS-guided fine-needle core liver biopsy sampling using a novel 19-gauge needle with modified 1-pass, 1 actuation wet suction technique. *Gastrointest Endosc*. 2018;87(2):469-75.

36. Sporea I, Popescu A, Focsa M, Becheanu G, Sirli R, Cornianu M, et al. Do the needle type and the operator experience influence liver biopsy specimen quality? *Cent Eur J Med*. 2013;8(5):669-73.

Appendix II: Tumor development study

Tumor (target) development and testing in a PVA liver phantom

1 Introduction

An additional study was performed to gain insight in the development of PVA tumors (targets) in PVA liver phantoms. The visibility of the targets, the forces that arise when puncturing the targets with a needle, and the displacement of the targets during puncturing with a needle were investigated during this study.

2 Materials and Methods

In the following section a detailed description will be given concerning the materials that were used for the experiment, the experimental set-up and the method that was used in conducting the experiment.

2.1 Materials

Different specimens, instruments and equipment were needed for these experiments to succeed and to get results concerning the visibility of the targets with ultrasound, needle forces during puncturing of the targets, and displacement of the targets during puncturing.

2.1.1 Specimens

Four different targets were made with SELVOL™ Polyvinyl Alcohol (Sekisui Specialty Chemicals America, Dallas, Texas) and coolant (G12/G12+, Protecton, Veldhoven, The Netherlands) with different conditions:

- 4% mass percentage PVA
- 4% mass percentage PVA and 1% mass percentage silica gel 60 (Merck KGaA, Darmstadt, Germany)
- 8% mass percentage PVA
- 8% mass percentage PVA and 1% mass percentage silica gel 60 (Merck KGaA, Darmstadt, Germany)

Green food coloring was added to the mixture of each target giving them a green color. The mixtures were poured in four different pvc pipes creating cylindrical targets. The targets had one freeze-thaw cycle before they were placed in the same acryl case as



Figure 1: Placement 3 perpendicular rods above and beneath the targets to hold the targets in place. First: side view, Second: top view

mentioned in section 3.2.1.1 with dimensions 130mm x 130mm x 220mm. Three perpendicular rods were placed beneath the targets and three perpendicular rods were placed above the targets in order to hold the targets in place during the freeze-thaw cycles. Figure 2 shows how the targets were held in place. The mixture of the liver phantom that was poured in after placement of the targets was made with the same PVA particles and coolant as used for the targets. It contained 4% mass percentage PVA and underwent two freeze-thaw cycles. Red food coloring was added to the mixture of the liver phantom. The recipe that was needed to make the liver phantom and targets was the same recipe as used in section 3.2.1.1 except for the rpm of the magnetic stirrer when making the targets which was 400 rpm.

2.1.2 Instruments

The same straight 1.04mm (19G) nitinol stylet that was used in section 3.2.1.2 was used for the experiments that were performed in order to obtain results on the puncture forces and the displacement of the targets. No instruments were needed for the results on visibility of the four targets.

2.1.3 Equipment

An Ultrasound System (Phillips HD7 Diagnostic Ultrasound System, Bothell, Washington USA) was used to gain visual images of the targets inside the PVA phantom in order to get results on the visibility of the targets. This system was also used to place the nitinol stylet straight above the targets for the force measurements and to detect if the targets displaced inside the liver phantom when puncturing them with the nitinol stylet. A linear stage (PRO115, Aerotech Inc, Pittsburgh, PA, USA) was used to clamp the nitinol

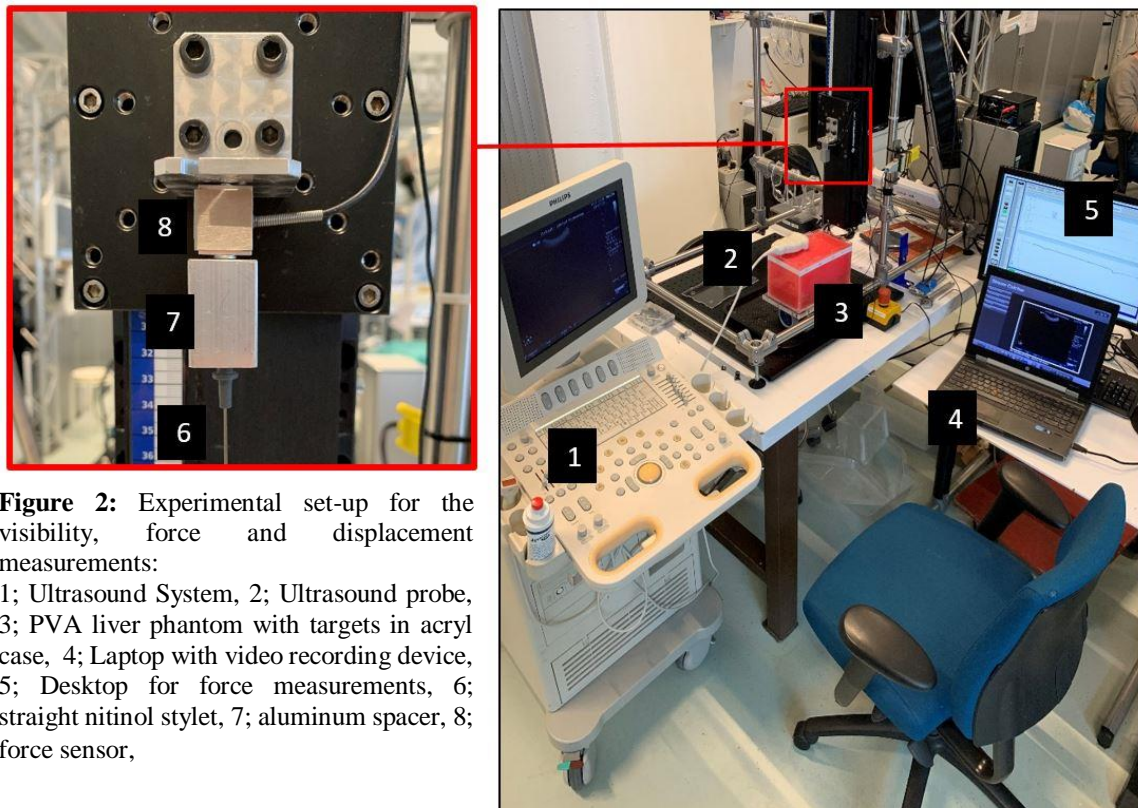


Figure 2: Experimental set-up for the visibility, force and displacement measurements:

1; Ultrasound System, 2; Ultrasound probe, 3; PVA liver phantom with targets in acrylic case, 4; Laptop with video recording device, 5; Desktop for force measurements, 6; straight nitinol stylet, 7; aluminum spacer, 8; force sensor,

stylet and insert it vertically into the PVA phantom with a constant speed and insertion depth. This was needed for both the force and displacement measurements. A force sensor (Futek Advanced Sensor Technology Inc., Irvine, California, USA) with a maximum capacity of 9N was placed between the needle and the attachment to the linear stage to measure the insertion forces and the forces that arise when transitioning between liver phantom and the targets. At last a video recording device (Stream catcher USB3HDCAP, Startech) was used to obtain images from the ultrasound system in order to determine the visibility of each target. It was also used to record videos of the ultrasound system during the displacement measurements to determine if the targets displace when puncturing them with the nitinol stylet. The visibility, force, and displacement measurements were combined into one experiment and figure 2 shows this combined experimental set-up.

2.2 Methods

A carefully designed experiment was set up to find results on the visibility of the targets in the PVA liver phantom, to obtain results on insertion forces and forces that arise when transitioning between the liver phantom and the targets, and to obtain results on the displacement of the targets when puncturing them.

2.2.1 Variables and constants

Visibility: The contrast-to-noise-ratio (CNR) is the dependent variable. For the independent variable the mass percentage of PVA and silica gel particles of the targets was taken, which differs between 4% and 8% for PVA particles and between 0% and 1% for silica gel particles. The only remaining constants are:

- Liver Phantom = 4% Polyvinyl Alcohol (PVA)
- Temperature = 20 °C
- Pressure = 760 mmHG
- Probe depth = 130 mm
- Gain = 232 dB

Force and displacement: The force and the displacement are the dependent variables. For the independent variable the mass percentage of PVA and silica gel particles of the targets was taken, which differs between 4% and 8% for PVA particles and between 0% and 1% for silica gel particles. The only remaining constants are:

- Velocity = 15 mm/s
- Liver Phantom = Polyvinyl Alcohol (PVA)
- Needle type = 19G straight nitinol stylet
- Initial distance = ±15 mm
- Insertion depth = 105 mm
- Angle of insertion = 90°
- Waiting time = 5 s
- Temperature = 20 °C
- Pressure = 760 mmHG

2.2.2 Experimental design

Visibility: For the visibility experiment two different mass percentages PVA (4% and 8%) and two different mass percentages silica gel (0% and 1%) were used for the

targets, which results in four different experimental conditions. Each experimental condition was tested for 15 repetitions. This makes a total of 60 repetitions for the four targets combined.

Force and displacement: The experiment that was designed to obtain results on forces and displacement of the targets also consisted of the four experimental conditions that are mentioned above. Each experimental condition was tested four times, resulting in a total of 16 repetitions for the four targets combined.

2.2.3 Experimental protocol

Visibility: To begin the experiment all materials and equipment must be in place. Set the probe depth of the ultrasound device to 130 mm. Connect the video recording device between the laptop and the ultrasound device. Position the probe on the PVA phantom and above the first target. Make a snapshot of the ultrasound screen with the video recording device. Repeat this 15 times while translating the probe over the entire target. Do this for all four targets.

Force and displacement: To begin the experiment all materials and equipment must be in place. Set the probe depth of the ultrasound device to 130 mm and the gain to 232 dB. Calibrate the force sensor that is placed between the nitinol stylet and the linear stage. Connect the video recording device between the laptop and the ultrasound device. Make sure that the nitinol stylet is aligned above the target with help of the ultrasound device. Place the probe on the PVA phantom in such a way that the stylet and target are clearly visible on the ultrasound device when puncturing the phantom and the targets. Let the linear stage then puncture the phantom for a depth of 105 mm until the target is reached. A signal is obtained in volts and displayed on the desktop. The entire puncture motion is captured by the video recording device and is transmitted to the laptop in order to determine the displacement of the targets during puncturing.

2.2.4 Data processing

Visibility: Contrast to noise ratio (CNR) is used to measure the visibility of each target. A larger CNR means that the PVA target is better distinguishable from the surrounding PVA liver phantom. A circle is placed on the PVA target and a circle with the same size is placed on the surrounding PVA. The CNR between the two circles is then calculated with Matlab. Figure 3 shows the PVA phantom with a target and both circles.

Force: The force sensor gave a signal in Volts, therefore it needed to be calibrated by hanging weights underneath the force sensor and note the number of volts for each weight. A formula could then be derived for the relation between volts and newton of the force sensor:

$$F = \frac{-V - 0.5749}{1.1825} \quad (1)$$

Thousand signals were given per second for a duration of 10 seconds, resulting in 10.000 values for the force which could be plotted in a graph with respect to the time.

Displacement: Each puncture with the needle was captured on video with the capture device. Displacement of the targets was checked by watching the videos after the experiments were executed.



Figure 3: Captured ultrasound image with the red circle indicating the PVA target and the blue circle indicating the surrounding PVA phantom. The CNR in this case was 7.9991

3 Results

3.1 Visibility of targets with ultrasound

The CNR of each target was calculated three times with Matlab for every picture and the average CNR of each picture was then calculated. The total average CNR was calculated by taking the average of the 15 pictures. Tables 1 till 4 show the average CNR per picture and the total average CNR for each target.

Table 1: CNR of target with 4% mass fraction PVA and no silica gel

	CNR pos 1	CNR pos 2	CNR pos 3	Average CNR
Picture 1	0,81107	0,78603	0,73519	0,77743
Picture 2	0,65773	0,59248	0,66302	0,63774
Picture 3	0,73528	0,85809	0,91948	0,83762
Picture 4	0,69590	0,70759	0,67319	0,69223
Picture 5	0,76453	0,71918	0,88988	0,79120
Picture 6	0,95242	0,70239	0,59313	0,74931
Picture 7	0,89383	0,93767	0,89071	0,90740
Picture 8	0,62820	0,50863	0,54634	0,56106
Picture 9	1,00830	0,86228	0,90834	0,92631
Picture 10	0,69551	0,67811	0,61220	0,66194
Picture 11	0,74868	0,59996	0,67350	0,67405
Picture 12	0,36929	0,30376	0,25289	0,30865
Picture 13	0,92821	0,73033	0,88156	0,84670
Picture 14	0,14899	0,14548	0,22733	0,17393
Picture 15	0,89113	0,71141	0,72018	0,77424
Total Average CNR				0,68799

Table 2: CNR of target with 4% mass fraction PVA and 1% mass percentage silica gel

	CNR pos 1	CNR pos 2	CNR pos 3	Average CNR
Picture 1	8,55010	8,05370	8,23940	8,28107
Picture 2	4,93620	5,06720	5,05880	5,02073
Picture 3	6,73920	7,11920	6,35310	6,73717
Picture 4	4,89680	6,34320	5,20940	5,48313
Picture 5	5,15940	4,46980	5,17420	4,93447
Picture 6	6,28910	6,14480	6,21710	6,21700
Picture 7	8,21890	7,72090	7,83850	7,92610
Picture 8	7,26890	7,54600	7,31080	7,37523
Picture 9	5,05460	5,18540	4,75660	4,99887
Picture 10	5,34950	4,72850	4,86200	4,98000
Picture 11	4,38160	4,56810	4,06150	4,33707
Picture 12	5,62990	4,97700	5,58400	5,39697
Picture 13	5,09640	5,01240	4,69570	4,93483
Picture 14	8,22390	8,00810	7,92160	8,05120
Picture 15	7,60500	7,78730	6,50380	7,29870
Total Average CNR				6,13150

table 3: CNR of target with 8% mass fraction PVA and no silica gel

	CNR pos 1	CNR pos 2	CNR pos 3	Average CNR
Picture 1	0,87259	0,72647	0,61219	0,73708
Picture 2	0,78074	0,78578	0,73799	0,76817
Picture 3	0,86171	1,14610	1,21690	1,07490
Picture 4	0,77802	0,95476	1,07730	0,93669
Picture 5	1,33150	1,43510	1,39310	1,38657
Picture 6	0,66007	0,67661	0,55784	0,63151
Picture 7	0,96695	0,95197	0,99621	0,97171
Picture 8	0,74291	0,84428	0,76796	0,78505
Picture 9	1,02190	1,16450	1,26500	1,15047
Picture 10	1,39050	1,45870	1,39270	1,41397
Picture 11	1,10600	1,17400	1,27460	1,18487
Picture 12	1,66460	1,52310	1,30140	1,49637
Picture 13	1,13240	1,05650	1,01970	1,06953
Picture 14	0,56462	0,52853	0,59398	0,56238
Picture 15	0,58566	0,56948	0,59812	0,58442
	Total Average CNR			0,98358

Table 4: CNR of target with 8% mass fraction PVA and 1% mass percentage silica gel

	CNR pos 1	CNR pos 2	CNR pos 3	Average CNR
Picture 1	5,63270	5,57590	5,69300	5,63387
Picture 2	7,12780	7,12380	6,48260	6,91140
Picture 3	6,61990	6,30450	6,68990	6,53810
Picture 4	7,11790	7,69340	6,58000	7,13043
Picture 5	6,27970	5,94750	6,24680	6,15800
Picture 6	6,30880	5,83530	6,64420	6,26277
Picture 7	7,17330	7,73900	7,11740	7,34323
Picture 8	5,83640	5,70950	6,64140	6,06243
Picture 9	8,21970	7,79070	8,61080	8,20707
Picture 10	1,22540	3,12150	2,84370	2,39687
Picture 11	7,29460	6,49010	7,19950	6,99473
Picture 12	6,34780	6,04650	6,57750	6,32393
Picture 13	5,31700	5,34660	5,15560	5,27307
Picture 14	6,25800	6,97790	7,41600	6,88397
Picture 15	7,83790	8,28610	8,19240	8,10547
	Total Average CNR			6,41502

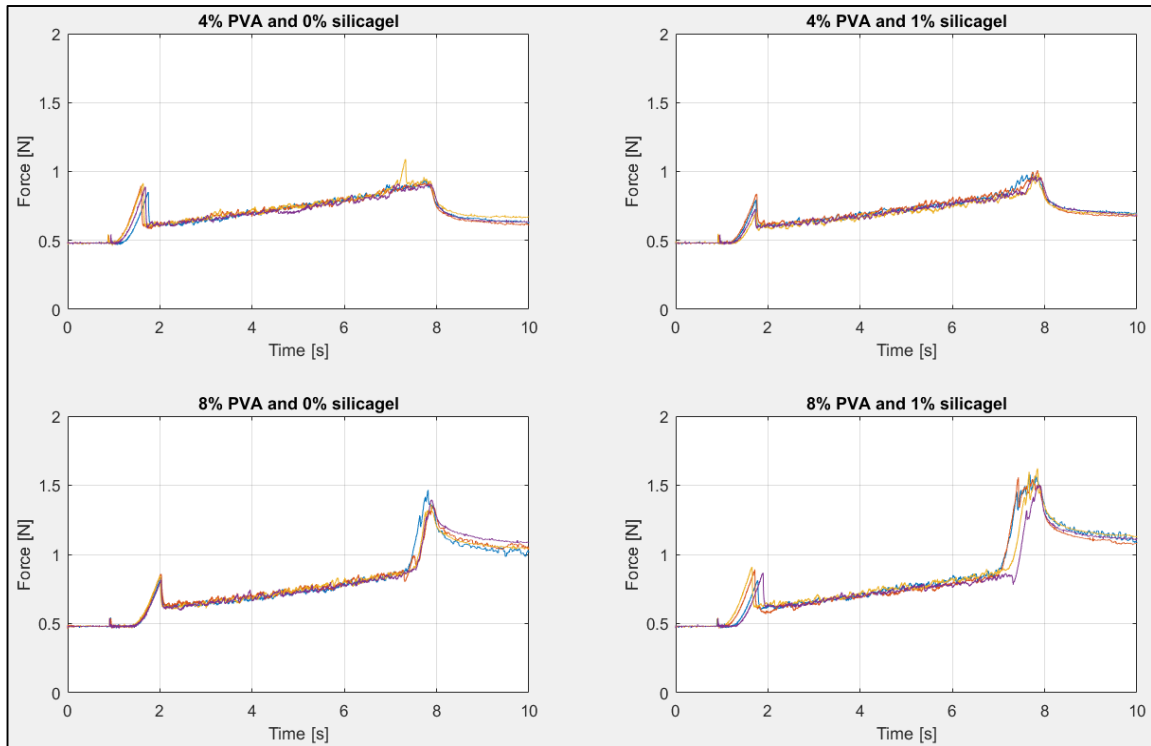


Figure 4: The four force measurements plotted in one figure over a period of 10 seconds for each of the four targets

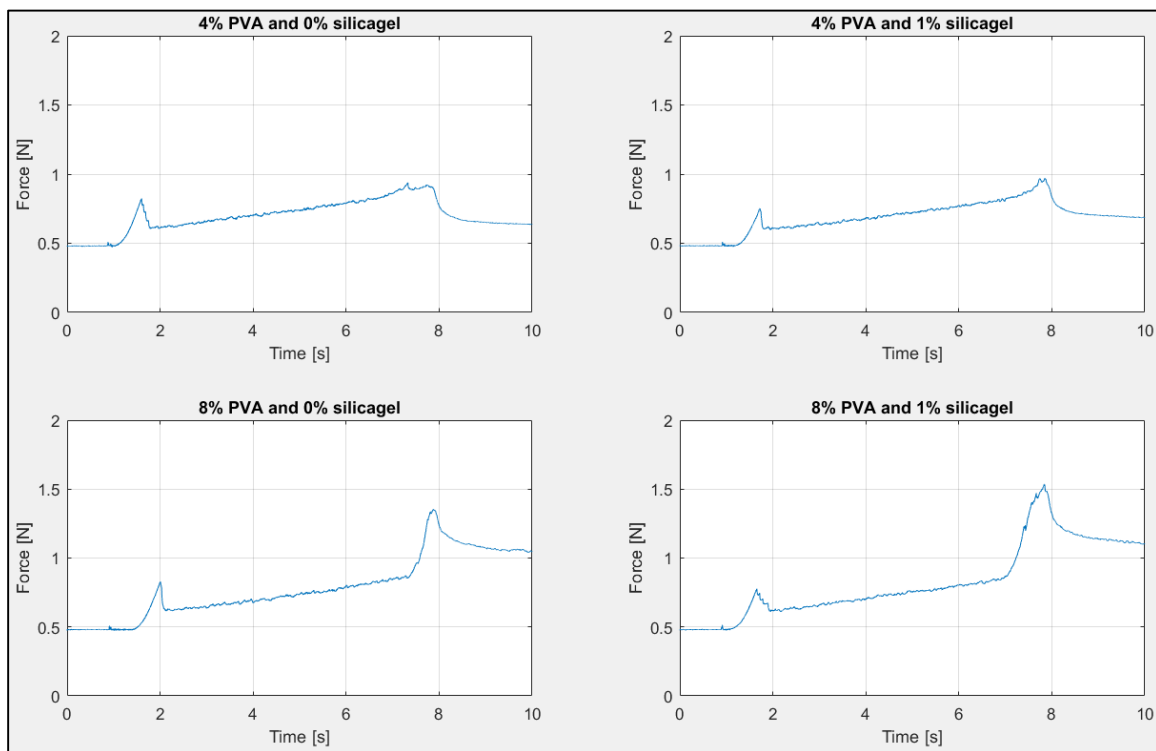


Figure 5: The average of the four force measurements plotted over a period of 10 seconds for each of the four targets

3.2 Needle forces during puncturing of the targets

A graph was made for each target, displaying the forces that were measured during puncturing of the PVA phantom and the PVA targets, for a total time of 10 seconds. Figure 4 displays the forces of the four measurements for each target and figure 5 displays the average force of the four measurements combined for each target. A peak starts to arise after about 1 second indicating that the PVA phantom is punctured at that time. Another peak arises between 7 and 8 seconds, indicating that the target is punctured. This happens for only three of the four targets that were tested. The 8% PVA targets shows a larger resistance compared to the 4% PVA targets. The 8% PVA with 1% silica gel target shows the largest resistance of the four targets.

3.3 Targets displacement during puncturing

No clear displacement of the targets is noticed on the captured videos of the insertions. More resistance is seen for the targets with a mass percentage PVA of 8% compared to the 4% mass percentage PVA targets, however the targets stay in place. The PVA phantom was cut in the longitudinal direction to see how much the targets were dissolved with the surrounding PVA phantom. Figure 6 shows a cross section of the PVA liver phantom.



Figure 6: Cross section of the PVA liver phantom with the targets (left to right) with 8% PVA and 0% silica gel, 8% PVA and 1% silica gel, 4% PVA and 0% silica gel, and 4% PVA and 1% silica gel.

4 Discussion

The goal of this study was to gain more insight in the development of PVA tumor targets with respect to the visibility of the targets, the forces that arise when puncturing the targets with a needle, and the displacement of the targets during puncturing with a needle were investigated during this study.

Results on the visibility of the four different targets show that adding silica gel to the PVA mixture rapidly increases the CNR and thereby the visibility of the targets with ultrasound imaging. A slight increase of the CNR is also seen when the mass percentage

of PVA particles in the mixture is doubled from 4% to 8%. Targets containing silica gel and a higher mass percentage of PVA are better visible with ultrasound imaging.

Results on the needle forces that occur when puncturing the PVA phantom and targets, show only one peak for the target containing 4% PVA and no silica gel and two peaks for the other three targets. This indicates that this target has emerged with the surrounding PVA (figure 6) and offers no resistance to the needle. The target with the 4% PVA and 1% silica gel shows a small second peak between 7 and 8 seconds, meaning that adding silica gel to the mixture offers more resistance to the needle. The targets with a mass percentage of 8% PVA show the largest peaks between 7 and 8 seconds. The 8% PVA with 1% silica gel target shows the largest second peak of the four targets. Tumors are cirrhotic and offer more resistance to the needle compared to healthy liver tissue, therefore a higher second peak corresponds better with the reality.

Results on the displacement show that there was no clear distinction between the targets with respect to the displacement of the target during puncturing. No displacement was seen for either of the four targets.

In conclusion, better visibility of the PVA target on ultrasound imaging and higher peak forces during puncturing of the target were associated with a higher mass percentage of PVA particles, compared to the surrounding PVA, and addition of silica gel to the mixture. No clear distinction between the targets with respect to the displacement of the target during puncturing was seen.

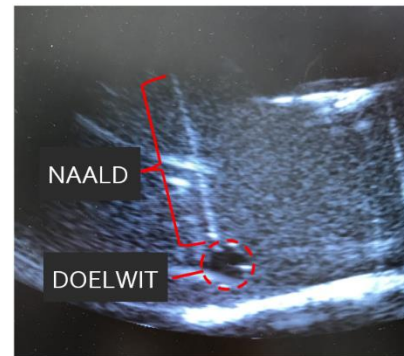
Appendix III: Manual user study

Handleiding experiment: Test procedure voor een stuurbare naald

Met dit experiment willen we de toepassing van een prototype van een stuurbare naald testen waarbij 2 verschillende taken aan bod komen:

- Naald in een recht pad naar doelwit
- Naald met een kromming naar doelwit

Deze taken worden elk 6 maal uitgevoerd waarbij een echoprobe (ultrasound) voor visuele informatie (figuur 1) zorgt tijdens het sturen. Deze probe is bevestigd aan de opstelling.



Figuur 1

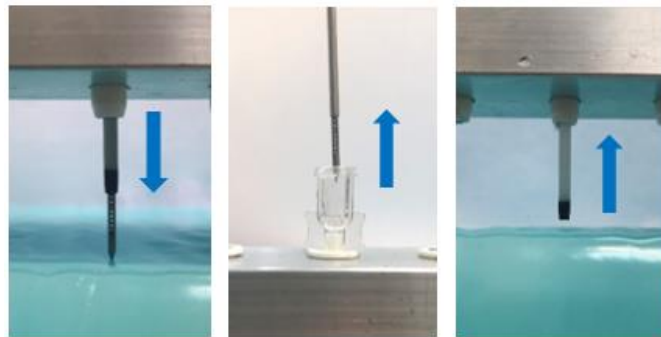
Kennismaking met instrument

Het is belangrijk dat het werkingsprincipe van het instrument duidelijk is. Voordat het experiment begint is er eerst tijd voor interactie met de verschillende onderdelen van het instrument.

- De hendel: rotatie hendel resulteert in rotatie naaldpunt (figuur 2)
- Luer lock: vergrendeling cannula met de stuurbare naald (figuur 4)



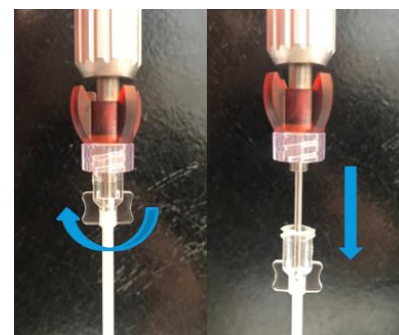
Figuur 2



Figuur 3

Stappenplan

1. Kennismaking met instrument
2. Plaats stuurbare naald door de trocar in het PVA sample (figuur 3 links)
3. Stuur naar doelwit met behulp van ultrasound
Stap 3 wordt getimed en tippositie genoteerd.
4. Losdraaien Luer lock (figuur 4)
5. Verwijderen stuurbare naald, cannula blijft in PVA sample (figuur 3 midden)
6. Plaats ablatie naald door cannula
Stap 4 t/m 6 worden getimed en de tippositie genoteerd.
7. Verwijderen ablatie naald (zie stap 5)



Figuur 4

8. Verwijderen cannula (figuur 3 rechts)

Het bepalen van de tippositie na de stappen 3 en 6 wordt gedaan om eventuele verplaatsingen van ten gevolgen van de instrumentenwissel te kwantificeren.

Vragenlijst

Wanneer de 3 verschillende taken uitgevoerd zijn zal een korte vragenlijst volgen om kennis te vergaren over de ervaring betreft de stuurbare naald en de opzet van het experiment.

Tijdsindeling

Taak	Tijdsduur
Kennismaking instrument + doornemen handleiding	5 minuten
Taak 1 (recht pad)	10 minuten
Gereedmaken opstelling taak 2	2 minuten
Taak 2 (gekromd pad)	10 minuten
Vragenlijst invullen	5 minuten
Totale tijdsduur	±30 minuten

Appendix IV: Informed consent (Dutch)

Toestemmingsverklaring formulier

Experiment stuurbare naald in fantoom lever weefsel

Verantwoordelijke onderzoeker: *Danny de Lange*

In te vullen door de deelnemer

Ik verklaar op een voor mij duidelijke wijze te zijn ingelicht over de aard, methode, doel en [indien aanwezig] de risico's van het onderzoek. Ik weet dat de gegevens en resultaten van het onderzoek alleen anoniem en vertrouwelijk aan derden bekend gemaakt zullen worden. Mijn vragen zijn naar tevredenheid beantwoord.

Ik stem geheel vrijwillig in met deelname aan dit onderzoek. Ik behoud me daarbij het recht voor om op elk moment zonder opgaaf van redenen mijn deelname aan dit onderzoek te beëindigen.

Naam deelnemer:

.....

Datum: Handtekening deelnemer:.....

In te vullen door de uitvoerende onderzoeker

Ik heb een mondelinge en schriftelijke toelichting gegeven op het onderzoek. Ik zal resterende vragen over het onderzoek naar vermogen beantwoorden. De deelnemer zal van een eventuele voortijdige beëindiging van deelname aan dit onderzoek geen nadelige gevolgen ondervinden.

Naam deelnemer:

.....

Datum: Handtekening deelnemer:

Appendix V: Questionnaire (Dutch)

Vragenlijst experiment stuurbare naald

Leeftijd:
Uw expertise binnen het Erasmus MC:
Voert u dit soort procedures uit in de praktijk?:
Jaren ervaring:

Prototype van een stuurbare naald	Scale				
	S L E C H T	GOED			U I T S T E K E N D
1. Het gewicht van de stuurbare naald is goed te hanteren tijdens het experiment	1	2	3	4	5
2. Het stuurmechanisme (hendel) en het ontkoppelen van het Luer lock zijn snel onder de knie te krijgen	1	2	3	4	5
3. Stuurbaarheid van de naald in het PVA sample	1	2	3	4	5
4. Verloop van de instrumentenwissel tijdens het experiment	1	2	3	4	5

Appendix V

5. Tijd die nodig is om de verschillende stappen van de taak te doorlopen (Lang = 1, kort = 5)	1	2	3	4	5
6. Integratie mogelijkheid van de stuurbare naald in een echte medische procedure	1	2	3	4	5
7. Algehele ervaring met het experiment	1	2	3	4	5
8. Wat mag de stuurbare naald kosten naar uw mening?					
9. Overige opmerkingen betreft de stuurbare naald					

Appendix VI: Raw data user study

Raw time results**Table 1:** *Raw time measurements subject 1*

Trial	Time till Target Steerable needle	Time till Target RFA needle	Total time
Straight trajectory			
1	16.53	27.83	44.36
2	23.06	31.46	54.52
3	17.36	29.55	46.92
4	18.65	30.08	48.73
5	13.59	23.54	37.13
6	16.29	40.60	56.90
Curved Trajectory			
1	89.13	41.96	131.09
2	43.00	35.46	78.46
3	30.80	23.92	54.72
4	25.96	29.06	55.02
5	15.73	27.83	43.56
6	12.58	33.90	46.48

Table 2: *Raw time measurements subject 2*

Trial	Time till Target Steerable needle	Time till Target RFA needle	Total time
Straight trajectory			
1	20.83	32.32	53.15
2	24.43	17.79	42.23
3	21.83	26.85	48.69
4	15.92	19.87	35.80
5	13.80	22.48	36.28
6	20.38	26.94	47.32
Curved Trajectory			
1	30.48	25.56	56.04
2	48.46	31.72	80.19
3	27.72	13.98	41.70
4	17.52	26.39	43.92
5	21.15	38.41	59.56
6	13.96	29.20	43.17

Table 3: *Raw time measurements subject 3*

Trial	Time till Target Steerable needle	Time till Target RFA needle	Total time
Straight trajectory			
1	48.42	27.36	75.78
2	31.82	23.83	55.66
3	10.35	24.81	35.16

Appendix VI

4	10.45	22.21	32.67
5	6.56	21.76	28.33
6	8.65	15.60	24.25
Curved Trajectory			
1	12.36	15.65	28.02
2	7.95	13.54	21.50
3	17.23	14.31	31.55
4	10.86	12.82	23.68
5	17.56	12.96	30.52
6	12.82	18.26	31.09

Table 4: Raw time measurements subject 4

Trial	Time till Target Steerable needle	Time till Target RFA needle	Total time
Straight trajectory			
1	6.40	36.86	43.26
2	6.39	35.30	41.69
3	7.80	27.12	34.92
4	8.49	17.73	26.23
5	6.68	17.78	24.46
6	6.12	17.94	24.06
Curved Trajectory			
1	51.20	33.95	85.15
2	9.28	41.43	50.72
3	10.26	25.99	36.26
4	19.82	22.49	42.32
5	7.52	20.73	28.25
6	8.12	25.04	33.16

Table 5: Raw time measurements subject 5

Trial	Time till Target Steerable needle	Time till Target RFA needle	Total time
Straight trajectory			
1	18.41	32.46	50.88
2	14.12	13.89	28.01
3	14.49	11.67	26.16
4	10.99	18.40	29.40
5	10.88	16.94	27.83
6	14.60	11.22	25.82
Curved Trajectory			
1	6.90	10.50	17.40
2	14.06	12.35	26.42
3	8.15	10.93	19.09
4	8.88	11.78	20.67
5	9.88	12.31	22.20
6	10.49	18.16	28.46

Table 6: Raw time measurements subject 6

Trial	Time till Target Steerable needle	Time till Target RFA needle	Total time
Straight trajectory			
1	30.48	33.28	63.77
2	10.93	25.53	36.47
3	16.83	21.80	38.63
4	19.29	26.57	45.87
5	15.49	16.57	32.06
6	14.16	15.19	29.35
Curved Trajectory			
1	10.79	17.81	28.60
2	59.19	17.93	77.12
3	21.56	17.50	39.07
4	33.46	11.83	44.80
5	11.92	18.11	30.03
6	28.75	16.24	44.99

Raw hit-miss results and number of trials

Table 7: Raw hit-miss measurements and number of trials for subject 1

Trial	Hit (1) or miss (0) steerable needle	Hit (1) or miss (0) RFA needle	# of trials
Straight trajectory			
1	NaN	NaN	NaN
2	1	1	1
3	1	1	1
4	1	1	1
5	1	1	1
6	1	1	1
Curved Trajectory			
1	NaN	NaN	NaN
2	1	1	4
3	1	1	1
4	1	1	1
5	1	1	1
6	1	1	1

Table 8: Raw hit-miss measurements and number of trials for subject 2

Trial	Hit (1) or miss (0) steerable needle	Hit (1) or miss (0) RFA needle	# of trials
Straight trajectory			
1	1	1	1
2	1	1	1
3	1	1	1
4	1	1	1
5	1	1	1
6	1	1	1

Appendix VI

Curved Trajectory			
1	NaN	NaN	NaN
2	NaN	NaN	NaN
3	1	0	2
4	1	1	1
5	1	1	1
6	1	1	1

Table 9: Raw hit-miss measurements and number of trials for subject 3

Trial	Hit (1) or miss (0) steerable needle	Hit (1) or miss (0) RFA needle	# of trials
Straight trajectory			
1	1	1	1
2	1	1	1
3	1	1	1
4	1	1	1
5	NaN	NaN	NaN
6	1	1	1
Curved Trajectory			
1	1	1	1
2	1	1	1
3	1	1	1
4	1	1	1
5	1	1	3
6	1	1	1

Table 10: Raw hit-miss measurements and number of trials for subject 4

Trial	Hit (1) or miss (0) steerable needle	Hit (1) or miss (0) RFA needle	# of trials
Straight trajectory			
1	1	1	1
2	1	1	1
3	1	1	1
4	1	1	1
5	1	1	1
6	1	1	1
Curved Trajectory			
1	1	1	3
2	1	1	1
3	1	1	1
4	1	1	1
5	1	1	1
6	1	0	1

Table 11: Raw hit-miss measurements and number of trials for subject 4

Trial	Hit (1) or miss (0) steerable needle	Hit (1) or miss (0) RFA needle	# of trials
Straight trajectory			
1	1	1	1
2	1	1	1
3	1	1	1
4	NaN	NaN	NaN
5	1	1	1
6	1	1	1
Curved Trajectory			
1	1	1	1
2	1	1	2
3	1	1	1
4	1	1	1
5	1	0	1
6	1	1	1

Table 12: Raw hit-miss measurements and number of trials for subject 4

Trial	Hit (1) or miss (0) steerable needle	Hit (1) or miss (0) RFA needle	# of trials
Straight trajectory			
1	1	1	1
2	1	1	1
3	1	1	1
4	1	1	1
5	1	1	1
6	1	1	1
Curved Trajectory			
1	1	1	1
2	1	1	3
3	1	1	1
4	1	1	1
5	1	1	2
6	1	1	1

Appendix VII: Raw data of cannula displacement study

Raw data for a straight trajectory**Table 1:** Raw data concerning the displacement and deflection of the nitinol cannula in both x- and y-direction for a straight trajectory

Insertion	Displacement cannula x-direction (mm)	Displacement cannula y-direction (mm)	Deflection cannula x-direction (mm)	Deflection cannula y-direction (mm)
PVA liver phantom #1				
1	0	0	0	2
2	0	0	1	0
3	0	0	2	1
4	1	0	3	0
5	0	0	2	-3
6	0	0	2	2
7	0	0	3	0
8	0	-1	3	1
9	0	0	3	2
10	0	0	3	0
11	0	1	1	1
12	0	0	2	0
13	0	0	2	0
14	0	0	3	-1
15	0	0	4	1
16	0	0	4	1
17	0	1	2	1
18	0	0	3	0
19	0	0	3	1
20	0	0	4	0
21	0	0	3	-3
22	0	0	3	-2
23	0	0	3	0
24	0	0	3	-1
25	0	0	4	1
PVA liver Phantom #2				
26	0	0	4	0
27	0	0	4	0
28	0	0	3	-2
29	0	0	4	-2
30	0	0	4	-2
31	0	0	4	0
32	0	0	3	-2
33	0	0	4	-1
34	0	0	4	1
35	0	0	4	0

36	0	0	2	0
37	0	0	3	-3
38	0	0	4	-1
39	1	-1	4	0
40	0	0	3	-1
41	0	0	4	-2
42	0	0	4	-2
43	0	0	3	0
44	0	0	4	-2
45	0	0	3	0
46	0	0	4	-3
47	0	0	4	-1
48	0	0	4	-1
49	0	0	4	-1
50	0	0	4	-2

Raw data for a curved trajectory

Table 1: Raw data concerning the displacement and deflection of the nitinol cannula in both x- and y-direction for a curved trajectory

Insertion	Displacement cannula x-direction (mm)	Displacement cannula y-direction (mm)	Deflection cannula x- direction (mm)	Deflection cannula y- direction (mm)
PVA liver phantom #1				
1	0	-1	0	21
2	0	-1	0	25
3	0	-2	0	24
4	0	-1	1	25
5	0	-1	0	24
6	0	-2	0	23
7	0	-1	0	24
8	0	-1	0	24
9	0	-2	0	25
10	0	-1	0	24
11	0	-1	1	24
12	0	-2	1	25
13	0	-1	0	24
14	0	-1	0	24
15	0	-1	0	24
16	0	-2	0	27
17	0	-2	0	26
18	0	-1	0	25
19	0	-2	0	26
20	0	-2	0	26
21	0	-1	0	25
22	0	-2	0	25
23	0	-2	0	25

Appendix VII

24	0	-1	0	24
25	0	-2	0	23
PVA liver Phantom #2				
26	0	-2	2	19
27	0	-2	2	26
28	0	-2	2	25
29	0	-2	2	26
30	0	-2	2	26
31	0	-1	2	24
32	0	-1	2	25
33	0	-1	2	25
34	0	-1	2	25
35	0	-1	3	25
36	0	-2	2	26
37	0	-1	2	25
38	0	-2	2	26
39	0	-1	1	25
40	0	-1	2	24
41	0	-1	2	25
42	0	-1	2	24
43	0	-2	3	26
44	0	-1	2	26
45	0	-1	2	26
46	0	-2	2	26
47	0	-1	2	26
48	0	-1	2	25
49	0	-1	3	25
50	0	-1	3	25